AFRL-VA-WP-TR-2002-3032

CORROSION MORPHOLOGY IN LAP JOINTS

Gerhardus H. Koch
Steve E. Styborski

CC Technologies Laboratories, Inc.
6141 Avery Road
Dublin, OH 43016

JUNE 2000

Final Report for 01 April 1999 – 31 May 2000

Approved for public release; distribution is unlimited.

AIR VEHICLES DIRECTORATE
AIR FORCE RESEARCH LABORATORY
AIR FORCE MATERIEL COMMAND
WRIGHT-PATTERSON AIR FORCE BASE, OH 45433-7542

NOTICE

USING GOVERNMENT DRAWINGS, SPECIFICATIONS, OR OTHER DATA INCLUDED IN THIS DOCUMENT FOR ANY PURPOSE OTHER THAN GOVERNMENT PROCUREMENT DOES NOT IN ANY WAY OBLIGATE THE US GOVERNMENT. THE FACT THAT THE GOVERNMENT FORMULATED OR SUPPLIED THE DRAWINGS, SPECIFICATIONS, OR OTHER DATA DOES NOT LICENSE THE HOLDER OR ANY OTHER PERSON OR CORPORATION; OR CONVEY ANY RIGHTS OR PERMISSION TO MANUFACTURE, USE, OR SELL ANY PATENTED INVENTION THAT MAY RELATE TO THEM.

THIS REPORT IS RELEASABLE TO THE NATIONAL TECHNICAL INFORMATION SERVICE (NTIS). AT NTIS, IT WILL BE AVAILABLE TO THE GENERAL PUBLIC, INCLUDING FOREIGN NATIONS.

THIS TECHNICAL REPORT HAS BEEN REVIEWED AND IS APPROVED FOR PUBLICATION.

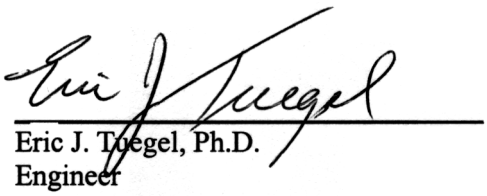

Eric J. Tuegel, Ph.D.
Engineer
Aircraft Structural Integrity

James W. Rogers, Major, USAF
Chief
Analytical Structural Mechanics Branch

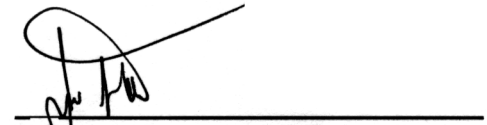

Jeffrey S. Turcotte, Lt. Col., USAF
Chief
Structures Division

Do not return copies of this report unless contractual obligations or notice on a specific document require its return.

REPORT DOCUMENTATION PAGE

Form Approved
OMB No. 0704-0188

1. REPORT DATE *(DD-MM-YY)*	2. REPORT TYPE	3. DATES COVERED *(From - To)*
June 2000	Final	04/01/1999 – 05/31/2000

4. TITLE AND SUBTITLE
CORROSION MORPHOLOGY IN LAP JOINTS

5a. CONTRACT NUMBER
F33601-96-D-J017

5b. GRANT NUMBER

5c. PROGRAM ELEMENT NUMBER
N/A

6. AUTHOR(S)
Gerhardus H. Koch
Steve E. Styborski

5d. PROJECT NUMBER
N/A

5e. TASK NUMBER
N/A

5f. WORK UNIT NUMBER
N/A

7. PERFORMING ORGANIZATION NAME(S) AND ADDRESS(ES)
CC Technologies Laboratories, Inc.
6141 Avery Road
Dublin, OH 43016

8. PERFORMING ORGANIZATION REPORT NUMBER

9. SPONSORING/MONITORING AGENCY NAME(S) AND ADDRESS(ES)
Air Vehicles Directorate
Air Force Research Laboratory
Air Force Materiel Command
Wright-Patterson AFB, OH 45433-7542

10. SPONSORING/MONITORING AGENCY ACRONYM(S)
AFRL/VASM

11. SPONSORING/MONITORING AGENCY REPORT NUMBER(S)
AFRL-VA-WP-TR-2002-3032

12. DISTRIBUTION/AVAILABILITY STATEMENT
Approved for public release; distribution is unlimited.

13. SUPPLEMENTARY NOTES
Report contains color.

14. ABSTRACT

This report describes a metallographic evaluation of lap joint corrosion as a function of location on a KC-135 aircraft. Sites for examination were selected on the fuselage and wings of the aircraft. Both two- and three-dimensional metallographic montages were prepared to characterize the corrosion damages and to determine the extent of the corrosion penetrations. Depending on the location on the airplane, different forms of corrosion were detected, which were dependent on the alloy microstructure. Examination of the microstructure and electrochemical tests provided insight into the distribution and type of corrosion observed in the lap joints.

15. SUBJECT TERMS
aluminum alloys, corrosion, aircraft lap joint

16. SECURITY CLASSIFICATION OF:			17. LIMITATION OF ABSTRACT:	18. NUMBER OF PAGES	19a. NAME OF RESPONSIBLE PERSON (Monitor)
a. REPORT	b. ABSTRACT	c. THIS PAGE			Eric Tuegel
Unclassified	Unclassified	Unclassified	SAR	44	19b. TELEPHONE NUMBER *(Include Area Code)* (937) 904-6772

HES&S 31-15093-1

Standard Form 298 (Rev. 8-98)
Prescribed by ANSI Std. Z39-18

TABLE OF CONTENTS

LIST OF FIGURES

LIST OF FIGURES **(continued)**

FOREWORD

This report presents the results of experimental studies that examined the microstructure and corrosion morphology at lap joints of aluminum alloy components of a KC-135 Air Force tanker. The work was performed by CC Technologies Laboratories, Inc. for the Air Force Research Laboratory (AFRL/VASM) through SelectTech Services Corporation Contract 3000-40-0153 (F33601-96-D-J017). The period of performance was from April 1999 through May 2000. Mr. Sean Coghlan of SelectTech Services was the Project Monitor.

SUMMARY

A large number of commercial and military aircraft have reached or exceeded their original design life, with a concomitant increase in maintenance and repair cost due to corrosion. A trend analysis of KC-135 depot maintenance recently conducted by the Air Force indicated an annual increase in maintenance core tasks of 10 percent over the past 10 years. In addition, corrosion is recognized to have a potential detrimental effect on the structural integrity of the aircraft. Corrosion in lap joints can lead to a decrease in strength as a result of loss in thickness, premature fatigue crack initiation caused by the formation of stress risers, and increased fatigue crack growth rates.

This paper describes a metallographic evaluation of lap joint corrosion as a function of location on a KC-135 aircraft. Sites for examination were selected on the fuselage and wings of the aircraft. Both two- and three-dimensional metallographic montages were prepared to characterize the corrosion damages and to determine the extent of the corrosion penetrations. Depending on the location on the airplane, different forms of corrosion were detected, which were dependent on the alloy microstructure. Examination of the microstructure and electrochemical tests provided insight into the distribution and type of corrosion observed in the lap joints.

1.0 INTRODUCTION

There is increasing concern about the potential effects of corrosion on the structural integrity of fuselage lap joints. Corrosion can lead to a decrease in strength due to the loss of lap joint skin thickness, early fatigue crack initiation due to the formation of stress risers, and increased fatigue crack growth rates. In fact, over the past several years, failures of lap joints have been reported on a number of commercial and military aircraft. However, these failures were generally attributed to multiple site damage (MSD) as a result of the formation of multiple fatigue cracks. The mode of corrosion in lap joints has generally been considered to be a uniform loss of material due to combined crevice and exfoliation corrosion, and no significance has been given to any other localized forms of attack, such as pitting and intergranular corrosion. Generally, the effects of corrosion on fatigue crack initiation and propagation in lap joints have not been considered because present nondestructive inspection (NDI) technologies are unable to detect all the corrosion before it affects the structural integrity of the lap joints. Thus, current aircraft maintenance guidelines for corrosion only consider thickness loss, which can affect the residual strength of the lap joint, and allow for a maximum loss in thickness of 10 percent within a single sheet before a repair must be made.

It is known that corrosion products, mainly $Al(OH)_3$, which form between the lap joints have a much larger volume than the aluminum alloy. A volume ratio for the aluminum hydroxide and aluminum of approximately 6.5 has been calculated [1]. The increased volume inside the lap joint can result in considerable deformation, or pillowing, of the skin between fasteners. It was further demonstrated that the resulting stress on the skin and fasteners could have a detrimental effect on the structural integrity of fuselage lap joints. A finite element model (FEM) was developed by Komorowski and coworkers [2, 3] to simulate the presence of the corrosion products and the loss of thickness, and to predict the stress distribution in lap joints. Also, fracture mechanics calculations were carried out to determine the effect of pillowing on the structural integrity of the lap joints [3, 4]. Koch et al. [5] have shown that in alloy 2024-T3, localized intergranular corrosion is often superimposed on the more visible exfoliation corrosion. Finite element analyses were performed to quantify the combined effects of thinning due to exfoliation, corrosion product formation resulting in pillowing, and localized intergranular corrosion. It was found that the stresses as a result of the localized corrosion could be sufficiently high that fatigue cracks could readily nucleate at these sites. In fact, using scanning electron microscopy (SEM), Komorowski et al. [6] showed extensive cracking in lap joints originating from corrosion of faying surfaces.

To determine if the types of corrosion, described in the earlier works, is present elsewhere on a typical transport airplane, a study was conducted to determine the types of corrosion on different structural components of such an airplane. Also, an attempt is made to correlate the observed corrosion with the environmental conditions inside the lap joint and the microstructures of the respective alloys of the joint.

2.0 OBJECTIVES AND TECHNICAL SCOPE

The objectives of this project were to characterize the corrosion morphology in wing and fuselage lap joints, and correlate the corrosion morphology with alloy type and microstructure. To meet these objectives, the project was divided into the following tasks:

Task 1: Characterization of Corrosion Morphology in Lap Joints
Task 2: Characterization of Microstructure
Task 3: Electrochemical Tests

3.0 APPROACH

3.1 Task 1: Corrosion Characterization

Sections from the following airframe components were selected for analysis:

- A section of the Al 7178-T6 inboard upper wing section at wing station 360 of the KC-135 (A/C 69149).
- A section of the Al 7178-T6 outboard upper wing section between wing station 733 188 and 643 50 of the KC-135 (A/C 69149).
- A section of the 2024-T3 fuselage near station BS420 and stringers S27 and S28 of the KC-135 (A/C 69149)
- A section of the 7075-T6 fuselage crown section between station BS916 and BS938 of the KC-135 (A/C 2668-019-B)

Figure 1 shows a schematic diagram of the upper wing skin of the KC-135 (A/C 69149), which was stationed for much of its life at Hickham AFB in Hawaii. The sections that were selected for metallographic examination were cut from the left inboard and left outboard wing.

The photographs in Figure 1 show cut sections viewed from the outside and inside of the wing. Clearly visible are the grindout marks at the fastener holes, which were made during maintenance to remove corrosion in these areas. Several metallographic cross sections were made in areas on the panels where significant corrosion was suspected. Selection of the areas for metallographic cross sectioning was guided by fastener holes and other locations with grindout indications. In areas where corrosion was observed on the metallographic cross sections, metallographic crosscuts were made so that three-dimensional montages of the corrosion damage could be produced.

A fuselage lap joint section was removed from the fuselage adjacent to a manhole at BS 420 and S28 of A KC-135 (A/C 69149) (see Figure 2). Again, several areas could be identified where the material was ground off in an apparent attempt to remove corrosion. Based on the location of the ground areas and the amount of corrosion found on the faying surface, areas for metallographic examination were selected.

Finally, a fuselage crown section of tapered Al 7075-T6 was removed between BS916 and BS938 of a KC-135 (A/C 2668-019-B). A photograph of this cut section is shown in Figure 3.

To examine for the presence of corrosion and corrosion products on the faying surface of the selected lap joint sections, the overlapping panels were separated carefully by drilling out the fasteners, removing any sealants, and pulling the panels apart. Care was taken not to damage the walls of the fastener holes. The Figures 1 and 2 clearly show the ground areas around some fastener holes on the exterior skin surface, as well as clear evidence of corrosion product on the faying surface. Based on the indications of grinding and corrosion at the fastener holes, metallographic cross sections were made through selected areas, such as shown in Figure 4. Figure 4 shows a schematic diagram of the outside upper wing skin lap joint section, with the metallographic cross sections indicated. The metallographic cross sections were ground and polished with colloidal silica to 0.05-μm finish and subsequently examined with an optical

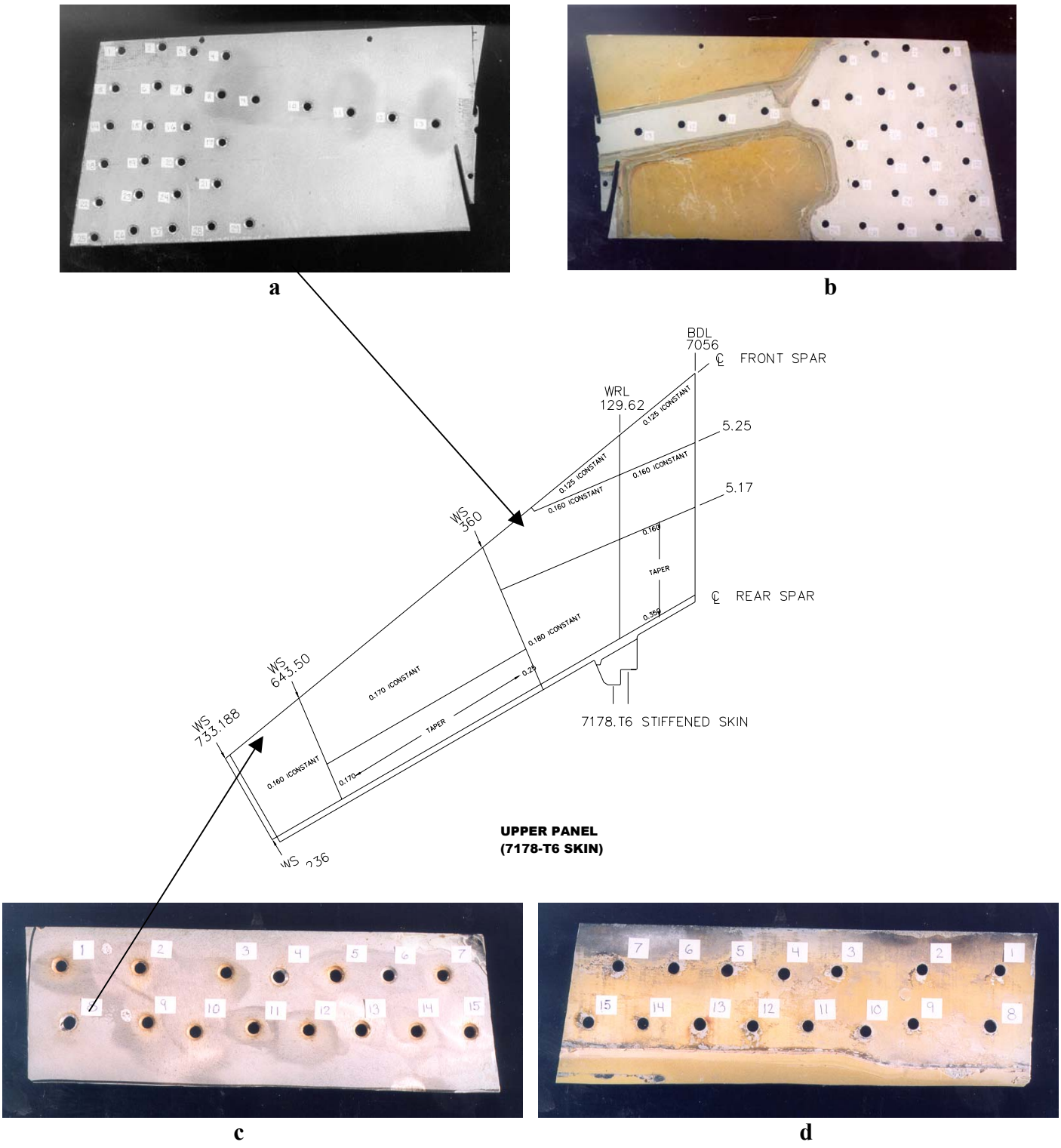

Figure 1. Schematic Diagram and Sections of Upper Wing Skin Panel of KC-135 (A/C 69149)
Photographs a and b show the exterior and faying surface of the inboard section.
Photographs c and d show the exterior and faying surface of the outboard section.

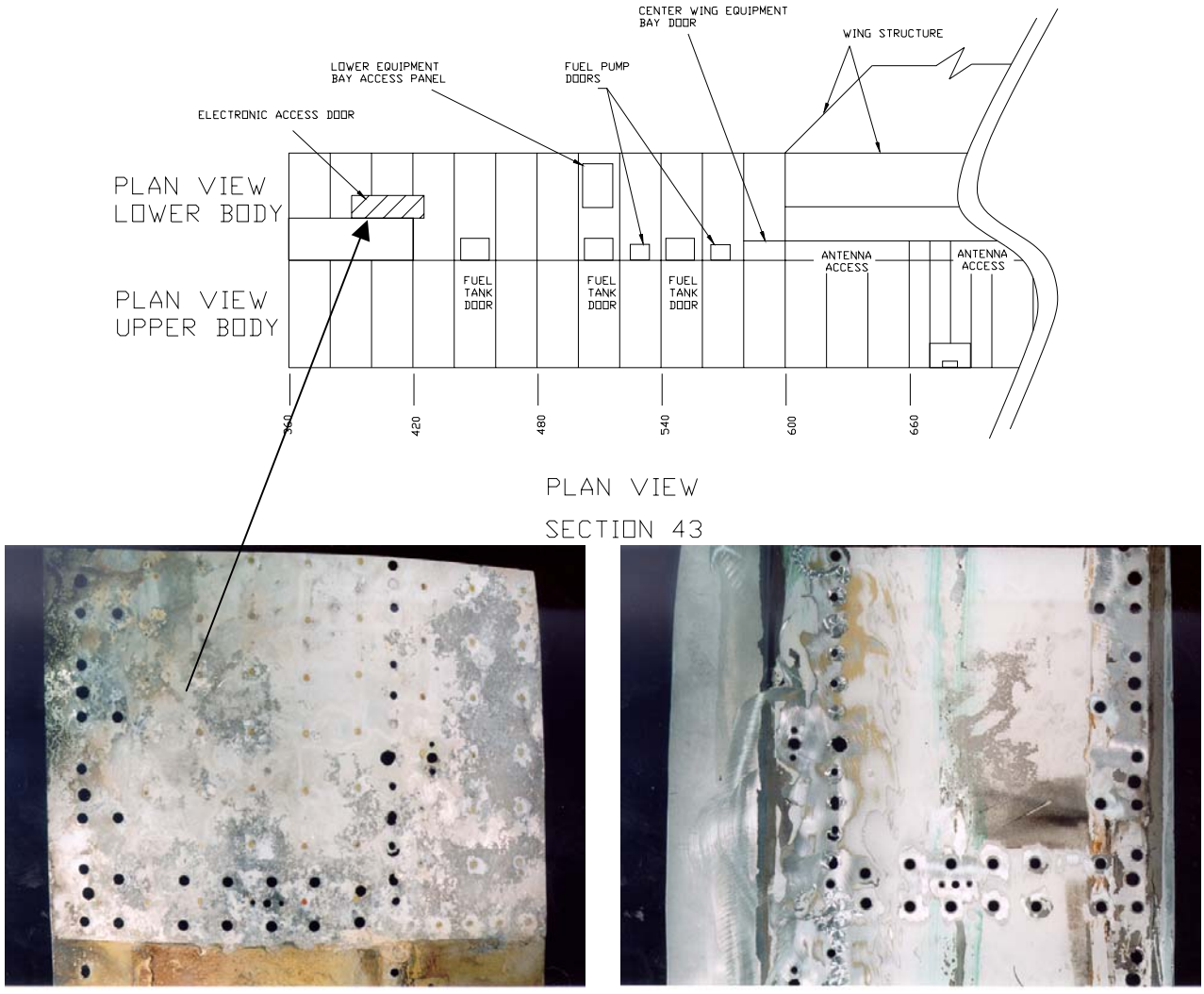

a **b**

Figure 2. Schematic Diagram of Fuselage Section of KC-135 (A/C 69149) with the Cutout Section Indicated by the Arrow
Photographs a and b show the matching faying surface and exterior surface of the section.

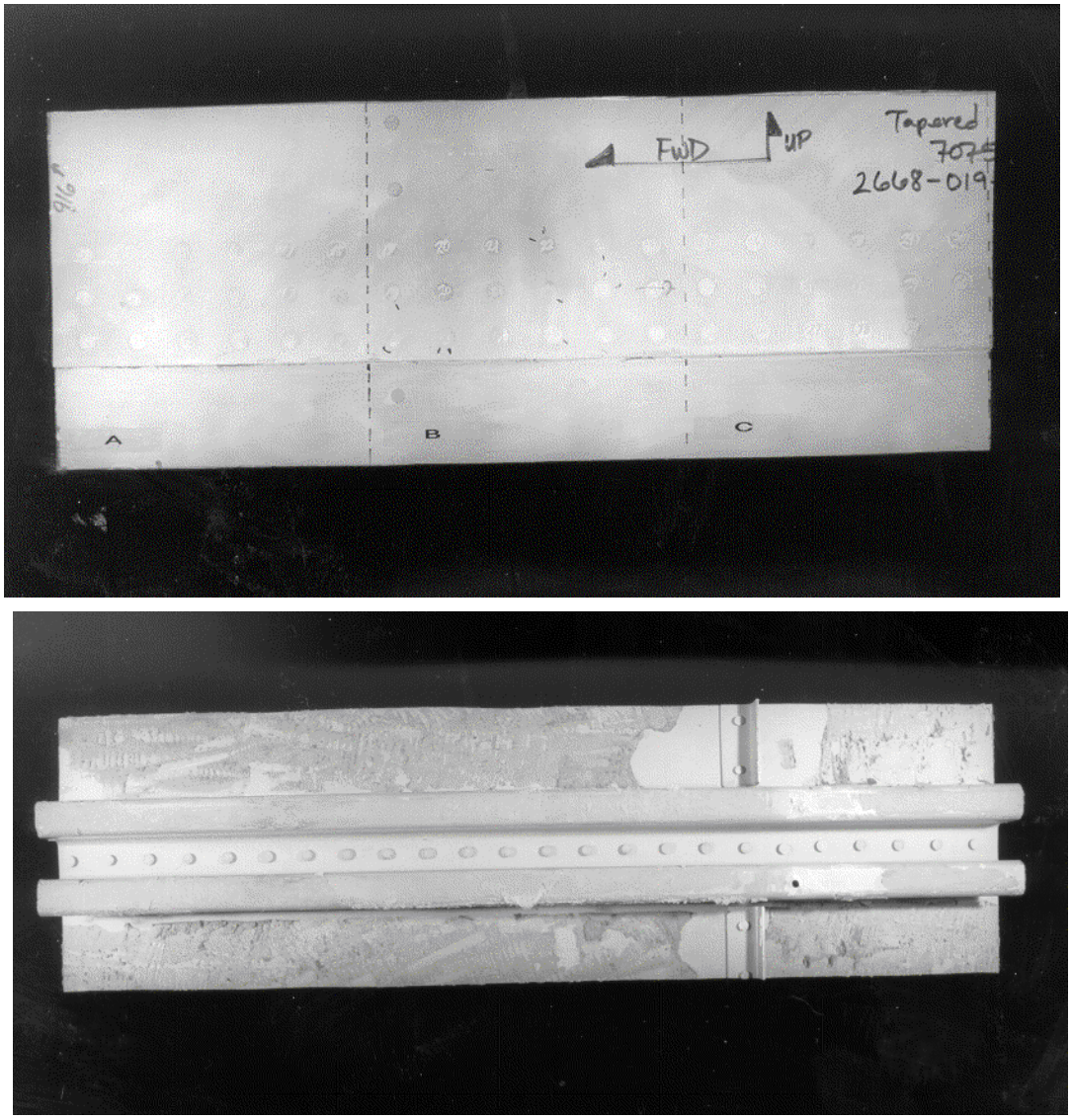

Figure 3. A Fuselage Crown Section Removed from an Area Between BS916 and BS938 of KC-135 (A/C 2668-19-B)

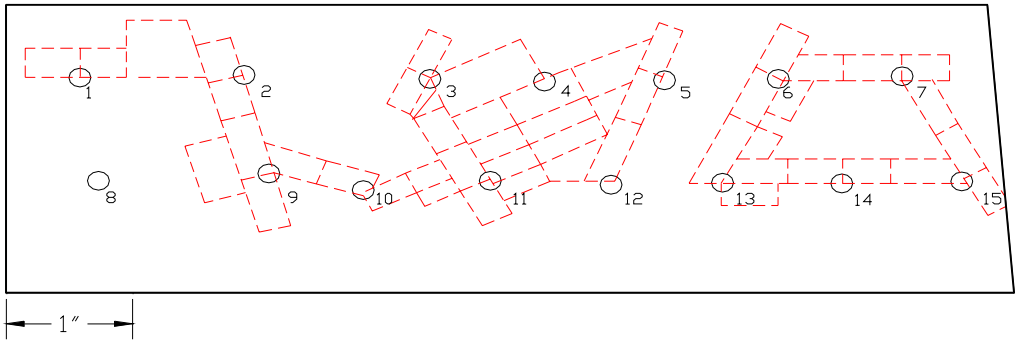

Figure 4. Schematic Diagram of Panel from Outboard Wing Section (see Figure 1, c and d), Showing Metallographic Cuts

microscope. In some cases, metallographic cross sections were made perpendicular to the original cross section in order to produce three-dimensional montages of the corrosion damage.

3.2 Task 2: Characterization of Microstructure

To find a correlation between the type of corrosion and the microstructure, metallographic cross sections were etched with nitric acid (25 percent HNO_3 at 70° C) or Kellers etchant. These etchants highlighted the grain and subgrain boundaries and made visible intermetallics such as $CuMgAl_2$ in the 2000 alloys and $AlMgZn_2$ in the 7000 alloys. These intermetallic compounds preferentially precipitate at grain boundaries and are known to create a susceptible path for corrosion attack; however, depending on heat treatment conditions, they also can precipitate intragranularly.

3.3 Task 3: Electrochemical Tests

It has been long suspected that the environment existing inside a lap joint varies with location. For example, both anodic and cathodic areas are known to exist on the faying surfaces of a corroding lap joint. The electrochemical potentials of these two areas are dictated by both material and environmental factors. Anodic polarization scans were performed on aluminum alloys 2024-T3, 7075-T6, and 7178-T6 that were removed from the KC-135 lap joint sections. Prior to testing, the clad layer was removed, and each specimen was abraded to 200 grit, degreased and rinsed with deionized water. Subsequently, the specimen was left in the test solution for a minimum of 8 hours to allow the surface to reach steady state conditions. The polarization scans were performed at ambient temperature in a deaerated 3 percent aqueous NaCl solution at a scanning rate of 10 mV/minute. The scan was started at starting approximately 50 mV more negative than the free corrosion potential (E_{cor}) of the specimen and was reversed at +1200 mV. Details of the test technique are given in ASTM Method G-61, “Standard Practices for Conducting Potentiodynamic Polarization Measurements for Localized Corrosion Susceptibility of Iron-, Nickel-, or Cobalt-Based Alloys.”

Based on the results of the potentiodynamic polarization tests, the specimens were held at different potentials in the deaerated 3 percent NaCl solution for up to 4 days. The

potentiostatically polarized specimens were metallographically sectioned, polished, and etched with Kellers etchant. Different types of corrosion attack resulted with the different potentials. The results were then correlated with those observed on the corroded lap joints.

4.0 RESULTS

4.1 Corrosion Characterization

The corrosion type in the different lap joints was characterized by optical and SEM. The lap joint sections were taken from the inboard and outboard upper wing, the fuselage, and the fuselage crown, as described earlier.

4.1.1 Upper Wing Skin Section

The inboard upper wing skin section lap joint showed no evidence of corrosion on the exterior surfaces other than the grindout marks (see Figure 1). Little corrosion was found on the faying surface. Upon careful examination of the fastener holes, metallographic cross sections were made at those locations where corrosion was visible. Figure 5 shows a three-dimensional montage of a section through the lap joint. It indicates the presence of only minor exfoliation near the exterior surface. Small corrosion penetrations also were observed on the walls of the fastener holes. Figure 6 shows an example of a fastener hole corrosion where both pitting and exfoliation were present just below the fastener hole chamfer.

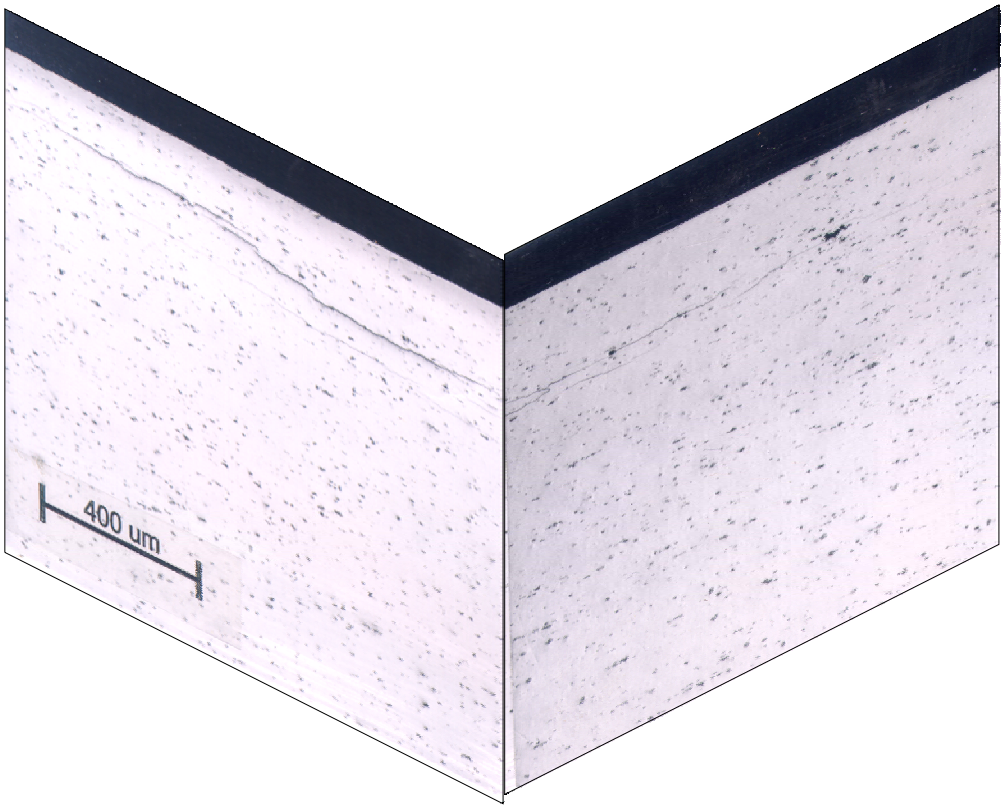

Figure 5. Three-Dimensional Image of Metallographic Cross Sections near Exterior of Inboard Wing Section Lap Joint

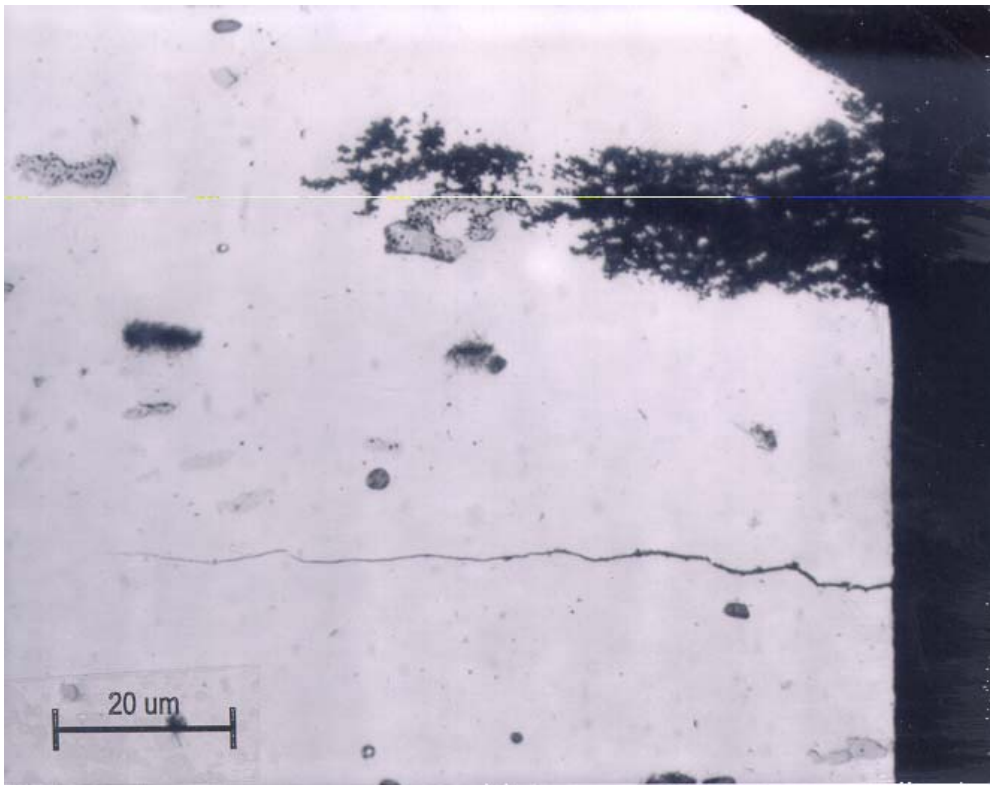

Figure 6. Optical Micrograph of Metallographic Cross Section Through Fastener Hole in Inboard Wing Section Lap Joint, Showing Minor Pitting and Exfoliation Corrosion

Although the outboard upper wing skin section lap joint did not show any sign of corrosion on the exterior and little corrosion on the faying surface, metallographic cross-sectioning revealed extensive exfoliation corrosion as well as pitting both at and in between the fastener holes. Figure 7 shows a schematic diagram of the exterior surface of the lap joint section and also optical of pitting and exfoliation corrosion in the areas indicated by arrows. Figure 8 shows a micrograph of a cross section through an area near fastener hole number 9 shown in Figure 7. Again pitting and exfoliation corrosion was found in the fastener hole walls and the top surface of the lap joint. The pitting corrosion showed some preferential dissolution that is characteristic for aluminum alloys (see Figure 9). Although the intergranular corrosion was extensive at some fastener holes, it appeared that little corrosion product had formed at the grain boundaries and, hence, the grains were not lifted. Because of the lack of corrosion product formation and grain exfoliation, detection, by any NDI technique, of this form of corrosion is expected to be difficult. The fact that intergranular attack was found under the grindout areas suggests that the NDI detection techniques following grindout had failed to find the corrosion damage. To gain insight in the morphology of the corrosion, three-dimensional montages were created by making perpendicular metallographic cross sections of the specimen. Examples of such three-dimensional montages in Figure 10 clearly demonstrate the fine nature of the intergranular corrosion and the lack of grain lifting or exfoliation. The micrographs further show that the corrosion was several grains deep in either direction, i.e., several 100 μm.

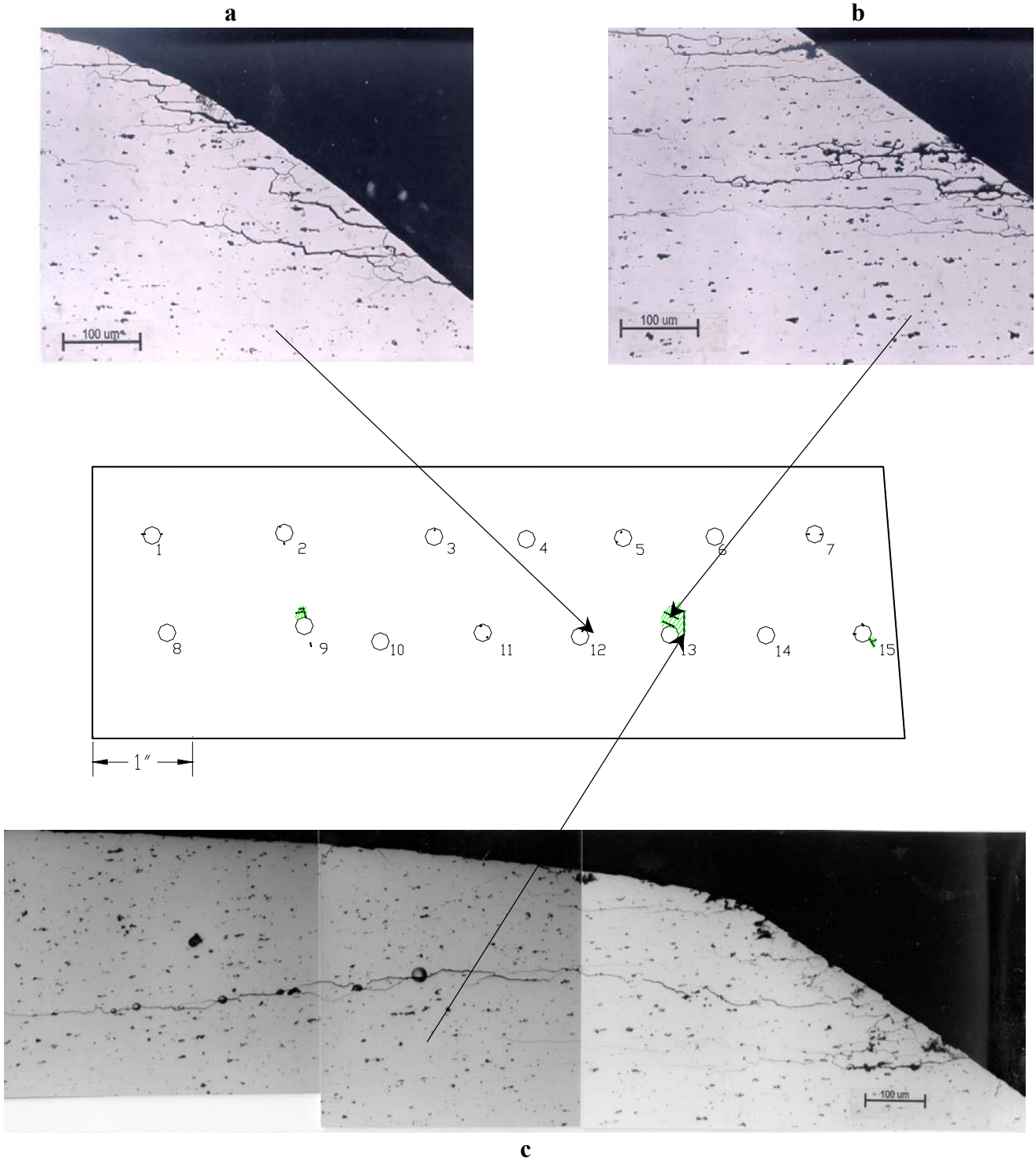

Figure 7. Schematic Diagram of Exterior Surface of Outboard Wing Lap Joint, Showing Areas of Exfoliation and Pitting Around the Fastener Holes

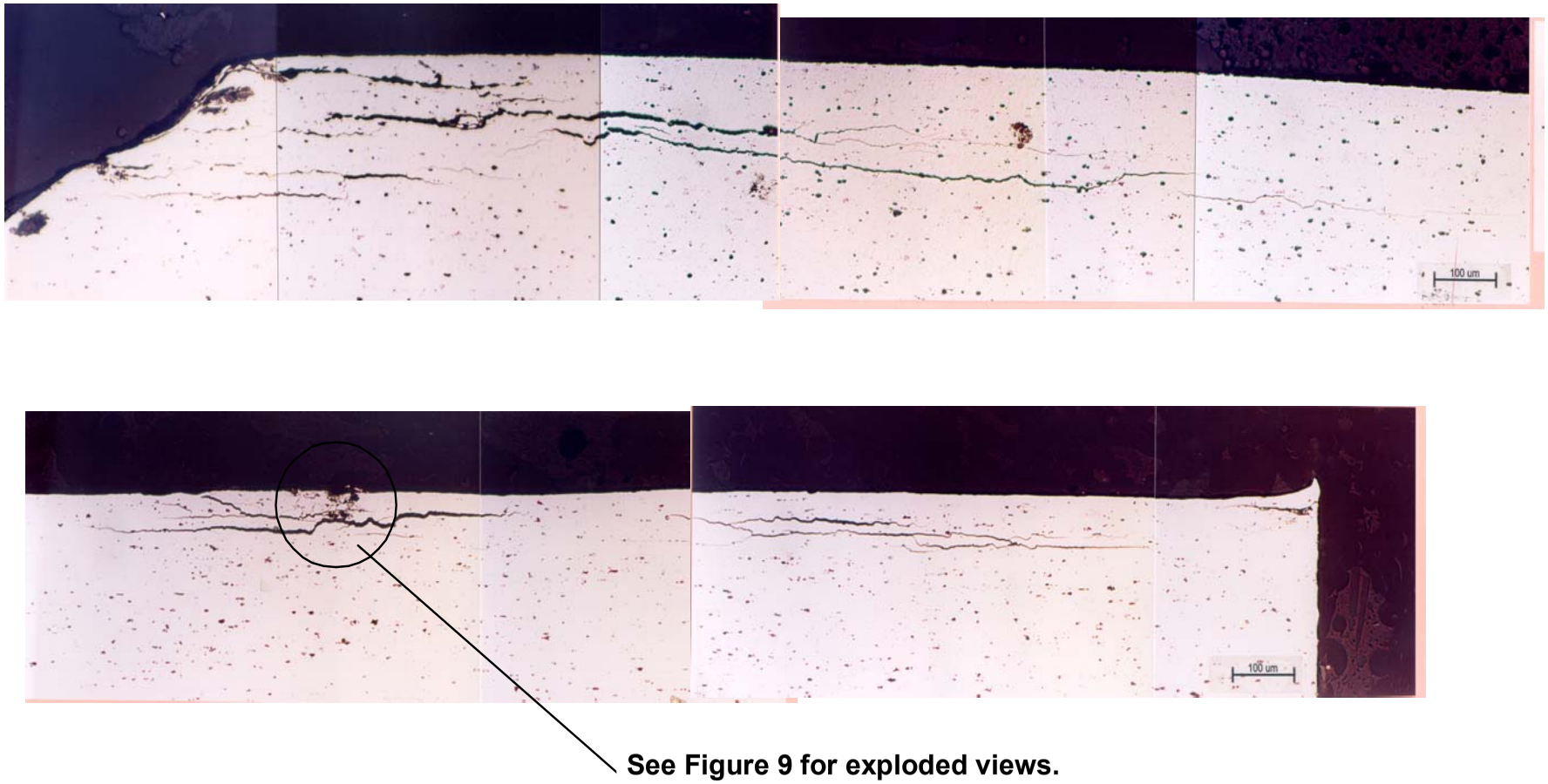

Figure 8. Optical Micrograph of Metallographic Cross Sections of Outboard Wing Lap Joint near Fastener Hole 9 in Figure 7

Exfoliation and pitting can be seen on the exterior of the upper wing skin.

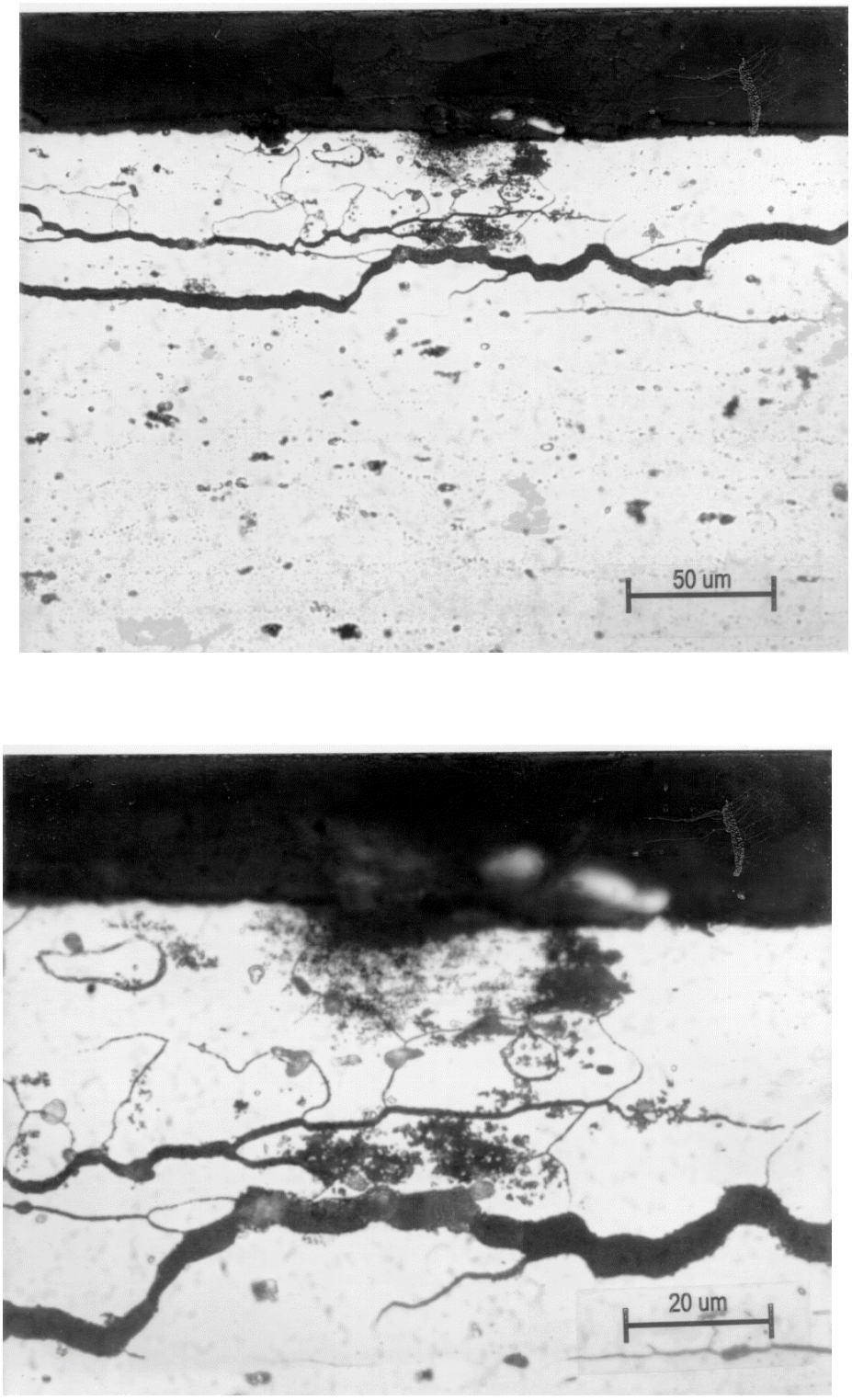

Figure 9. Details of the Pit Indicated in Figure 8

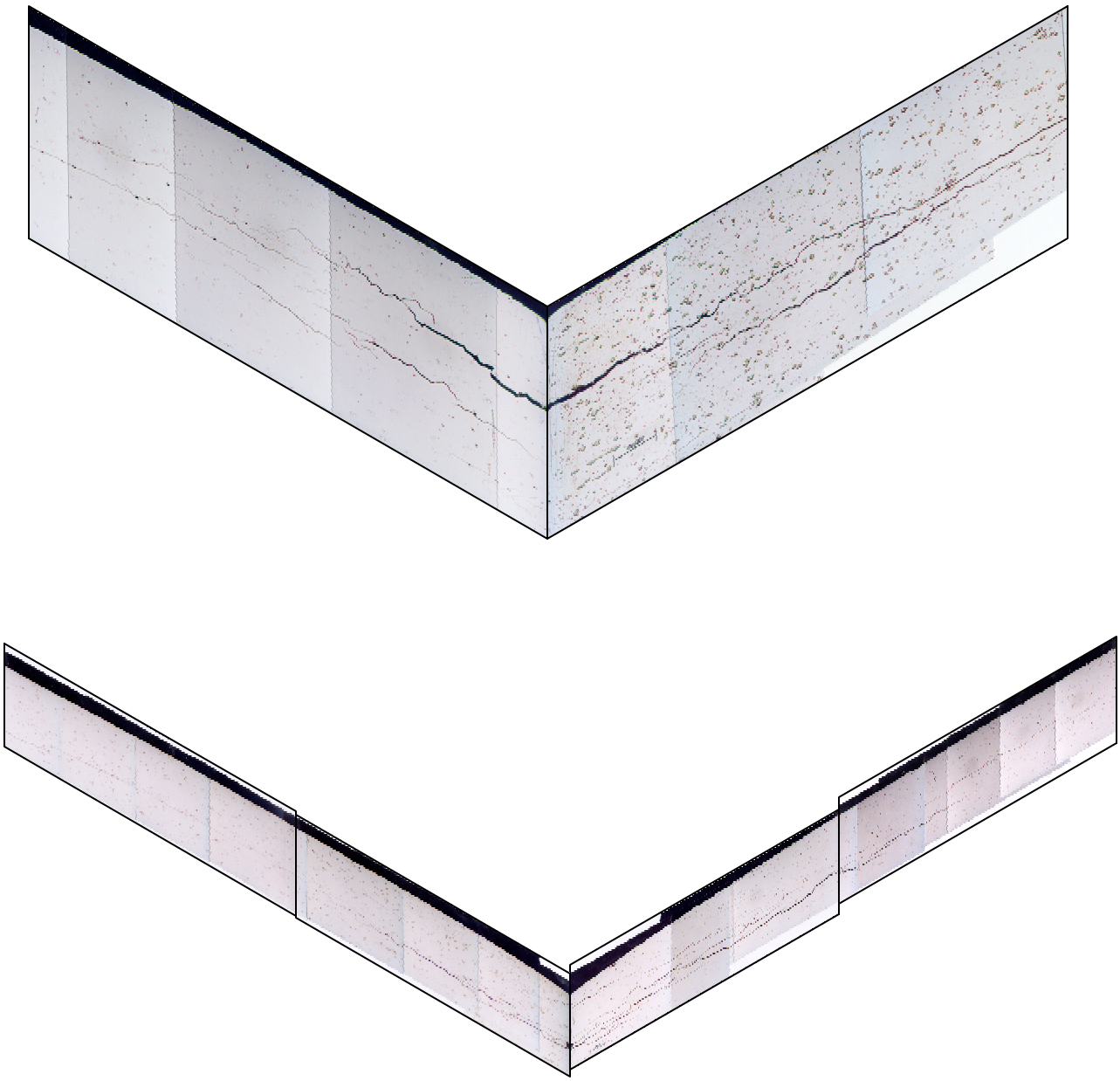

Figure 10. Three-Dimensional Images of Exfoliation Corrosion near Fastener Hole 13 in Figure 7

Figure 11 shows a schematic diagram of the faying surface of the lap joint, indicating that most of the corrosion occurred between the fastener holes. There was no evidence that the corrosion had originated from the fastener holes. When examining the corrosion on the faying surface, the morphology of the intergranular attack appears to be different from that observed near the exterior of the skin. The micrographs in Figure 11 show that voluminous corrosion products had formed along the grain boundaries, lifting up the grains and creating the so-called pillowing effect. Also, the micrograph in Figure 11b shows that after exfoliating, the grains continued to corrode by what appears to be a preferential dissolution process, forming the voluminous corrosion product ($Al(OH)_3$). To examine the extent of the intergranular attack, several metallographic cross cuts were made. Figure 12, which is a collage of optical micrographs, shows the extent and severity of exfoliation corrosion on the faying surface. Three-dimensional montages, such as in Figure 13, created from the metallographic crosscuts also demonstrate the large extent of the corroded area as well as a uniform depth of the corrosion attack of about 100 microns. The optical micrographs in Figures 12 and 13 further show definite pillow formation due to severe exfoliation corrosion.

In addition to exfoliation corrosion, it was found that at specific locations, pockets of intergranular corrosion were found extending deeper into the material. An example of this form of corrosion attack is given in Figure 14, which shows scanning electron micrographs of perpendicular metallographically prepared surfaces. The micrographs show clearly the formation of localized intergranular corrosion under the general exfoliation attack.

4.1.2 Fuselage Section

Examination of the 2024-T3 aluminum alloy lap joint sections in Figure 2 show the extensive grinding on the exterior surface and the presence of large amounts of corrosion products on the faying surface. In fact, when the lap joint panels were separated, powdery corrosion products that had build up in the joint fell out. Microscopic examination of metallographic cross section at various locations on the joint indicated that the alloy 2024 sheet contained clad on both sides and that the corrosion products had resulted from corrosion of the aluminum clad layer. Examination of several micrographs, such as shown in Figure 15, indicated extensive corrosion of the clad layer on the faying surface, but no corrosion in the 2024-T3 core material. It was further noted that corrosion of the clad was not uniform, but that shallow pits coalesced resulting in a scalloped surface texture.

4.1.3 Fuselage Crown Section

The alloy 7075-T6 crown section lap joint showed no visual evidence of corrosion on the exterior or faying surface of the lap joint (see Figure 3). Metallographic cross-sectioning indicated some corrosion near the edge of most of the fastener holes. An example is shown in Figure 16a, where pitting corrosion is seen on a metallographic cross section through a fastener hole. Further, extensive corrosion of the clad layer on the outside of the skin surface was observed (see Figure 16b). The micrographs clearly indicate that corrosion of the clad layer starts as localized pitting and extends across the clad surface.

Minor corrosion was found on the faying surface in the form of shallow pitting (see Figure 12c). It should be noted that there was no clad on the faying surface.

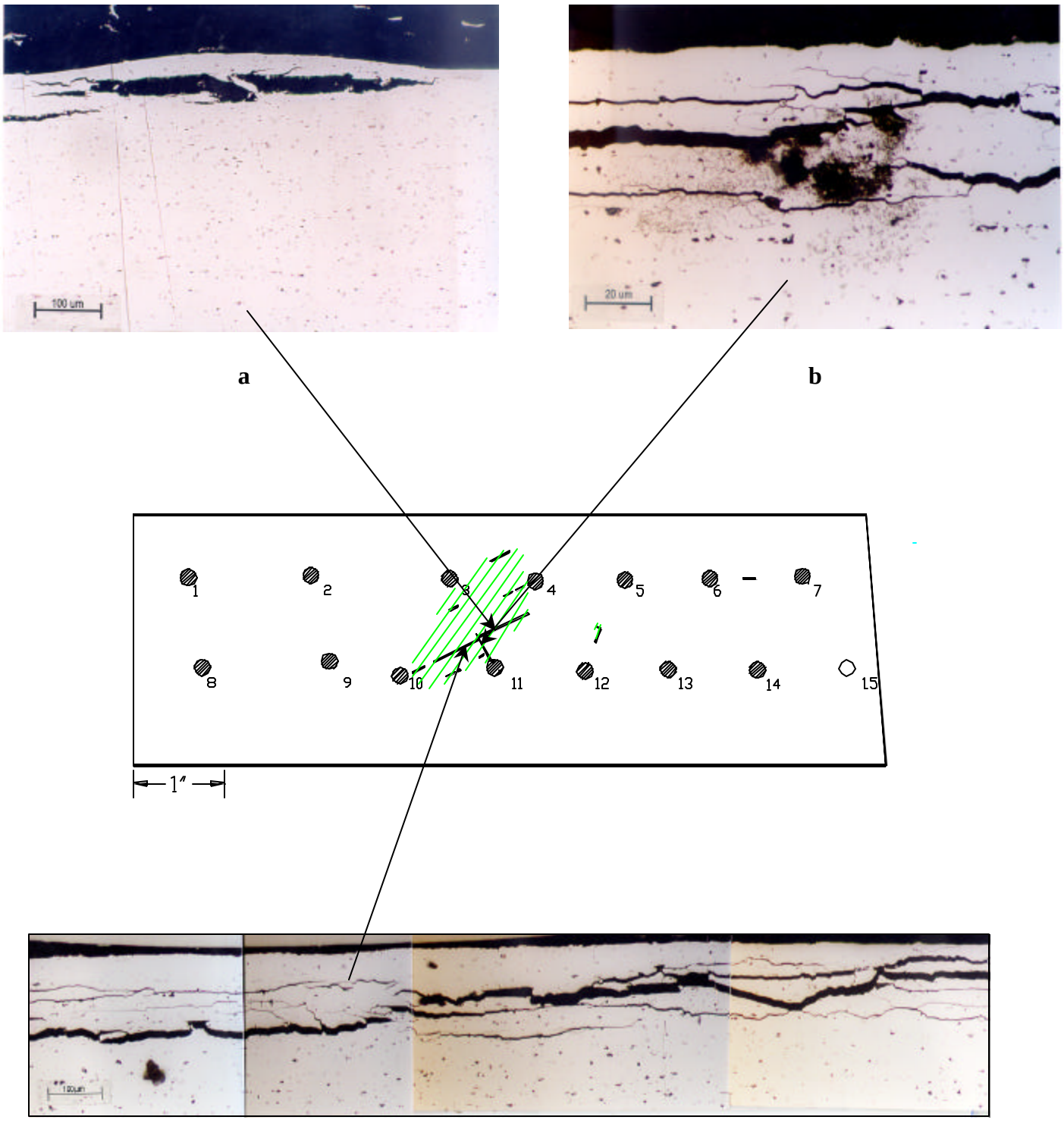

Figure 11. Schematic Diagram of Faying Surface of Outboard Wing Section, Showing Areas of Extensive Exfoliation Corrosion, Corrosion of the Exfoliated Grains and Pillowing

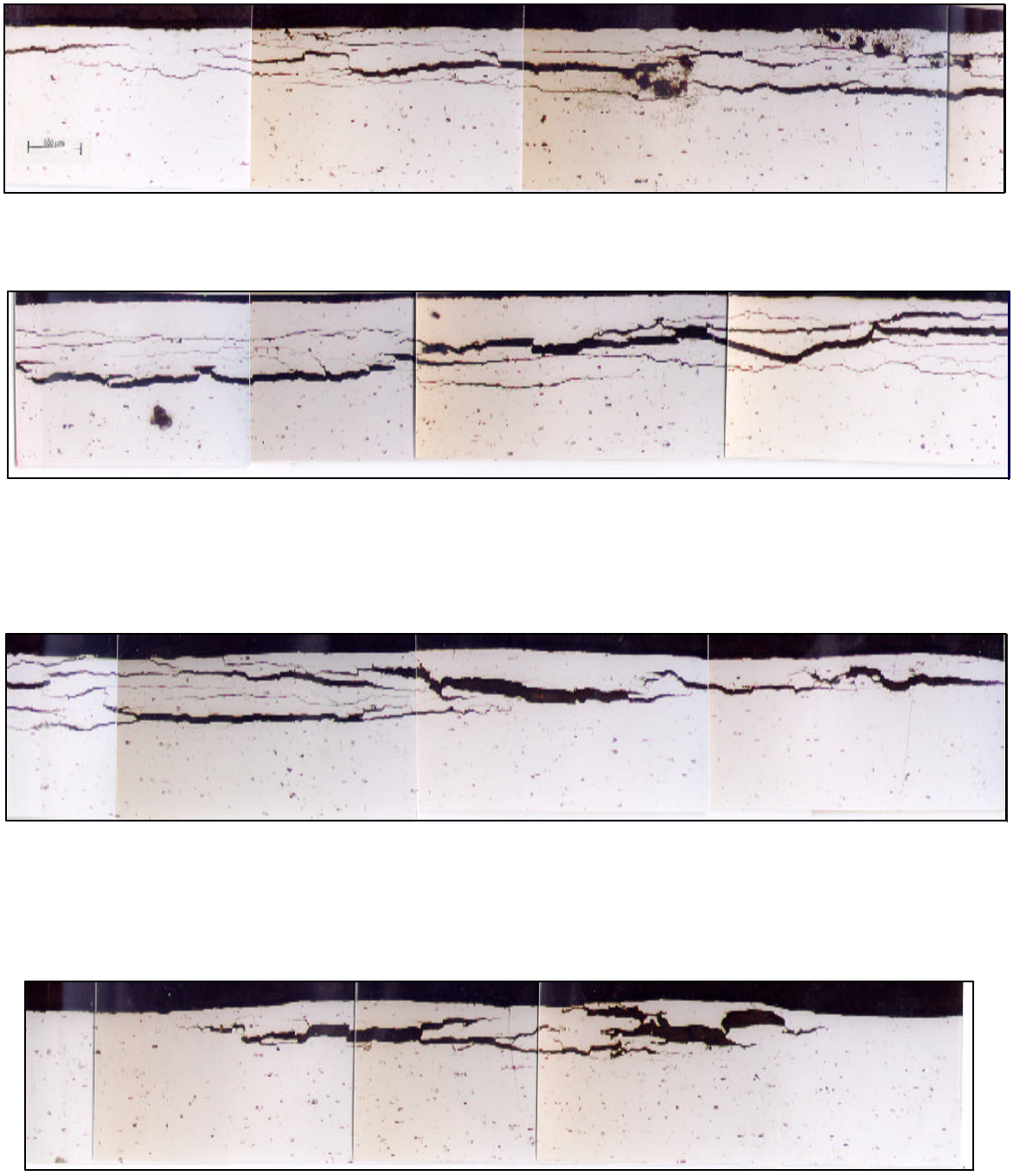

Figure 12. Optical Micrographs of Metallographic Cross Sections Through the Upper Wing Skin of the Outboard Wing Section, Showing Exfoliation and Blistering on the Faying Surface

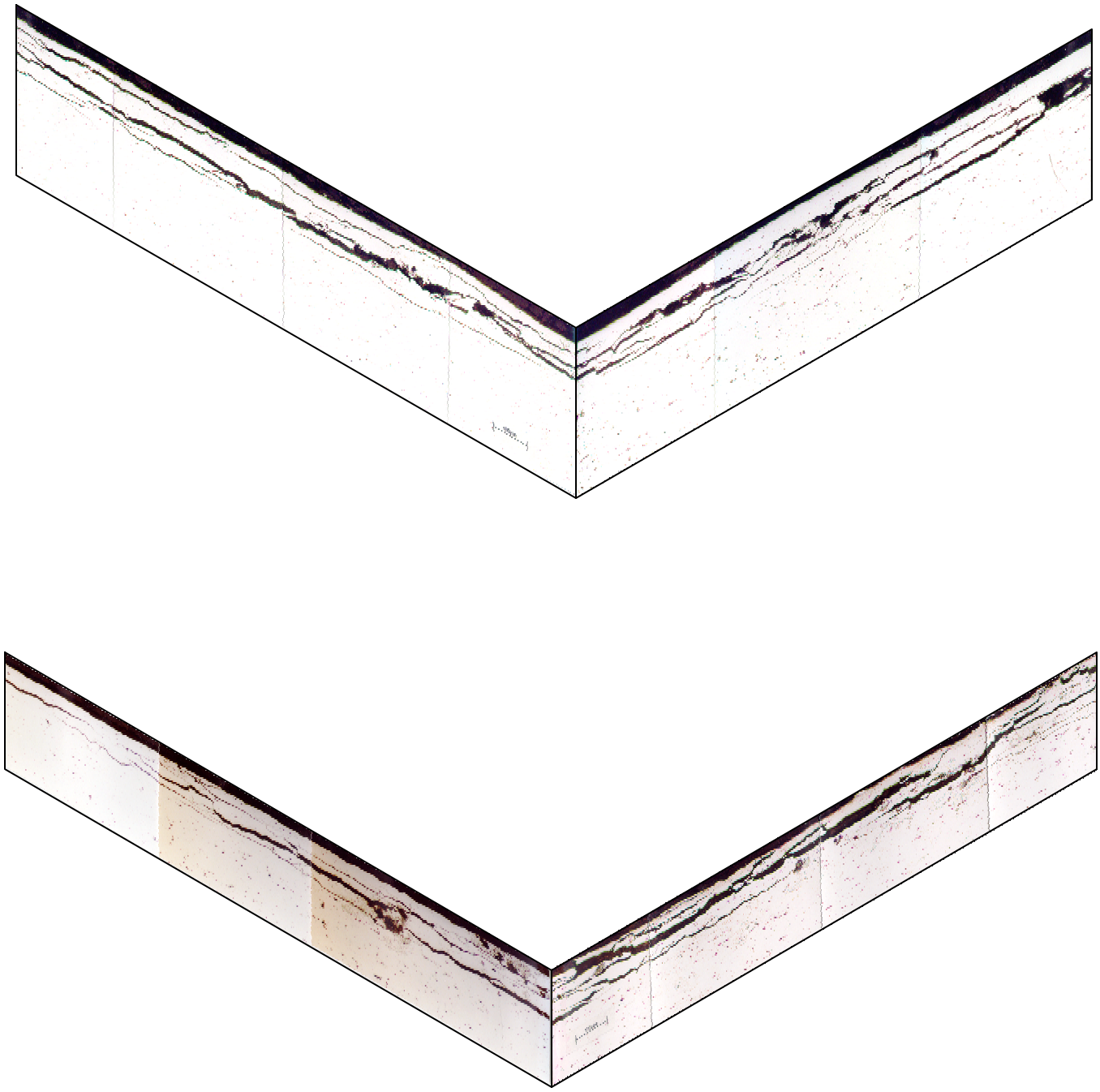

Figure 13. Three-Dimensional Images of Exfoliation Between Fastener Holes on the Faying Surface of the Outboard Wing Section, Showing Extensive Grain Lifting and Pillowing

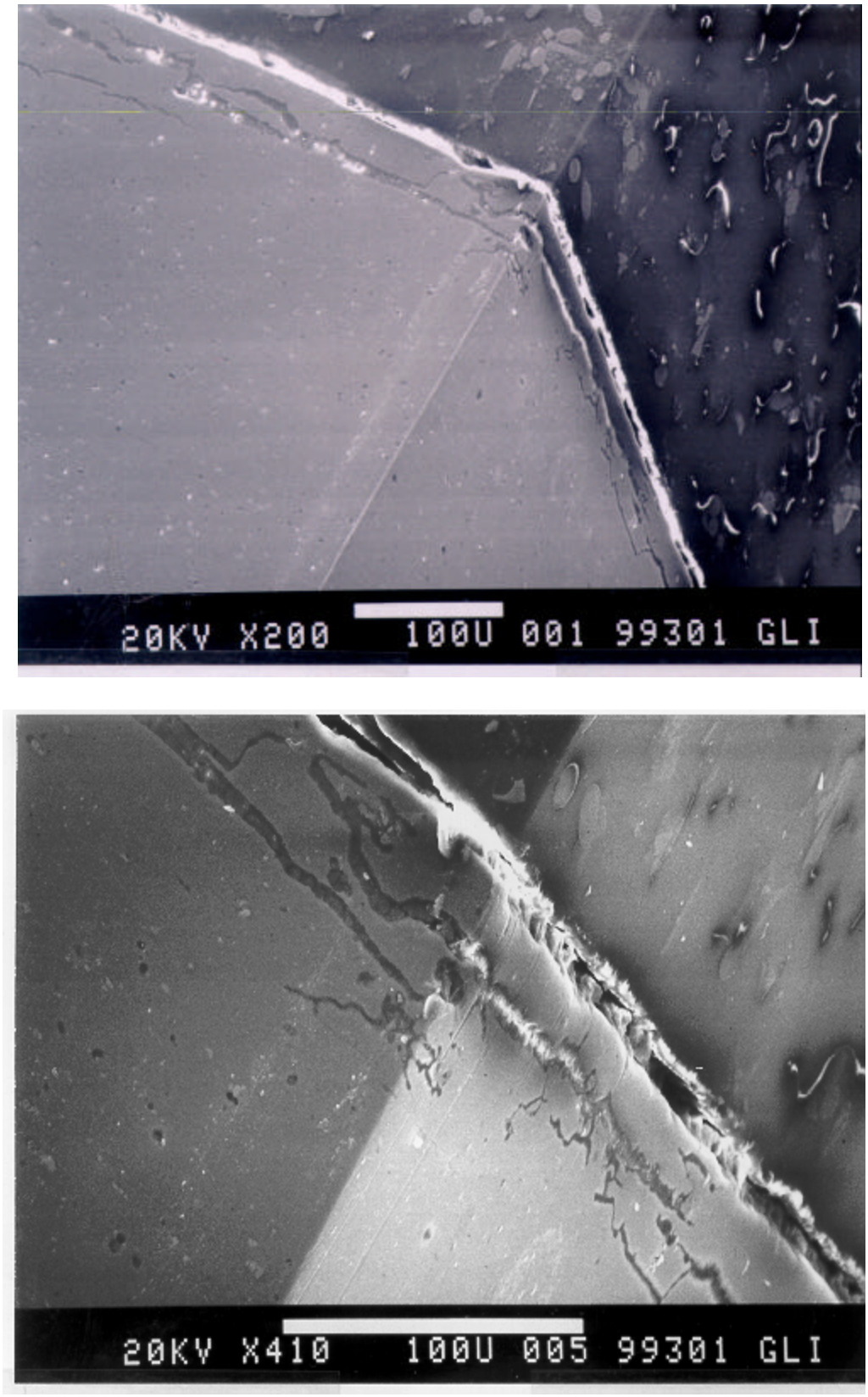

Figure 14. Scanning Electron Micrograph of Two Perpendicular Metallographic Cross-Sections of Outboard Wing Section, Showing Exfoliation and Intergranular Attack

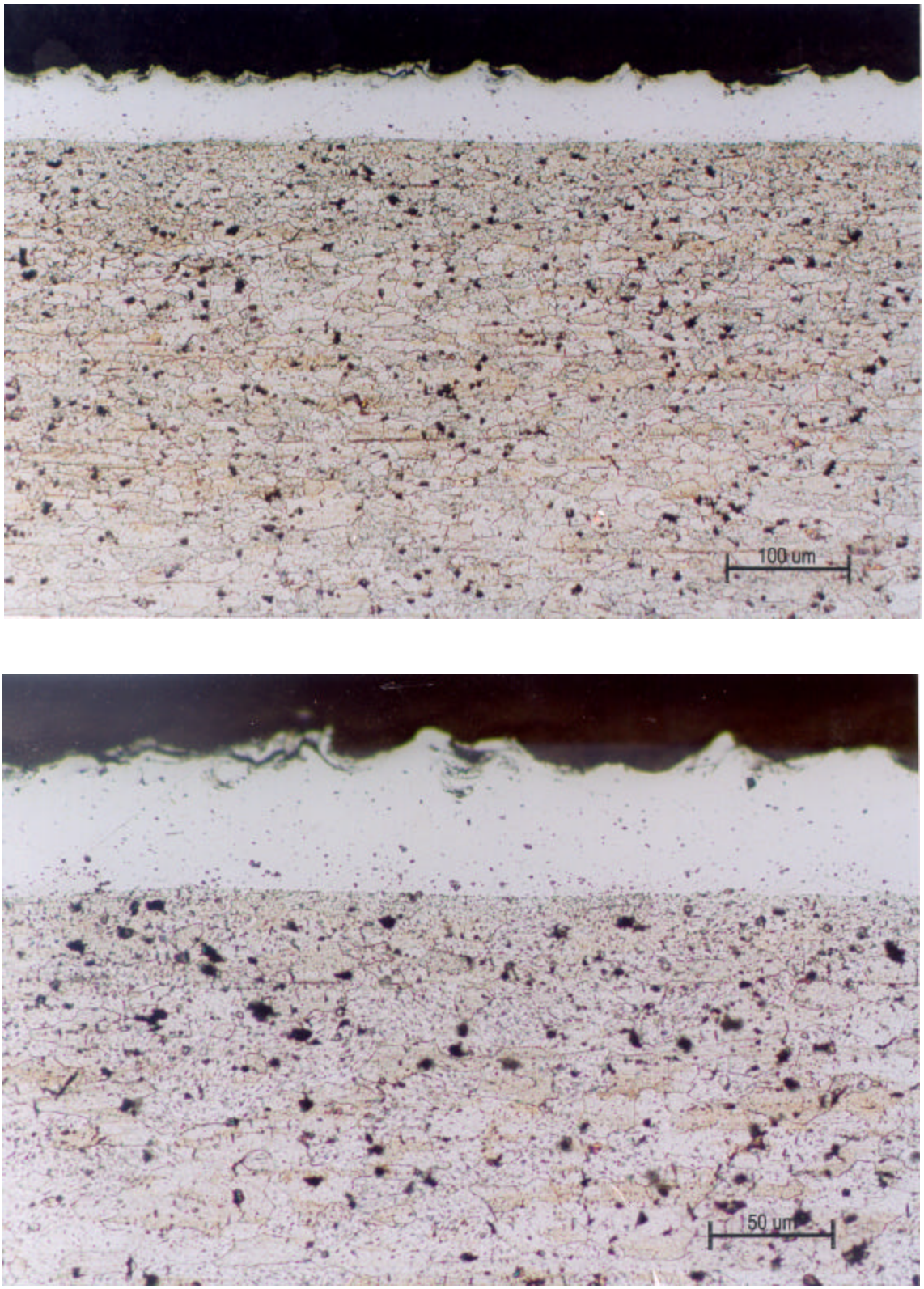

Etchant: Kellers

Figure 15. Optical Micrographs of Metallographic Cross Sections Through Aluminum Alloy 2024-T3 Fuselage Lap Joint, Showing Pitting on the Clad Faying Surface

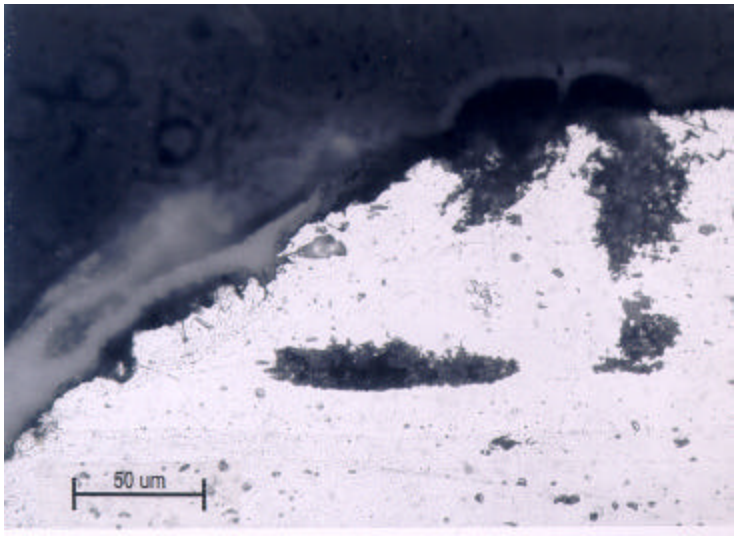

a

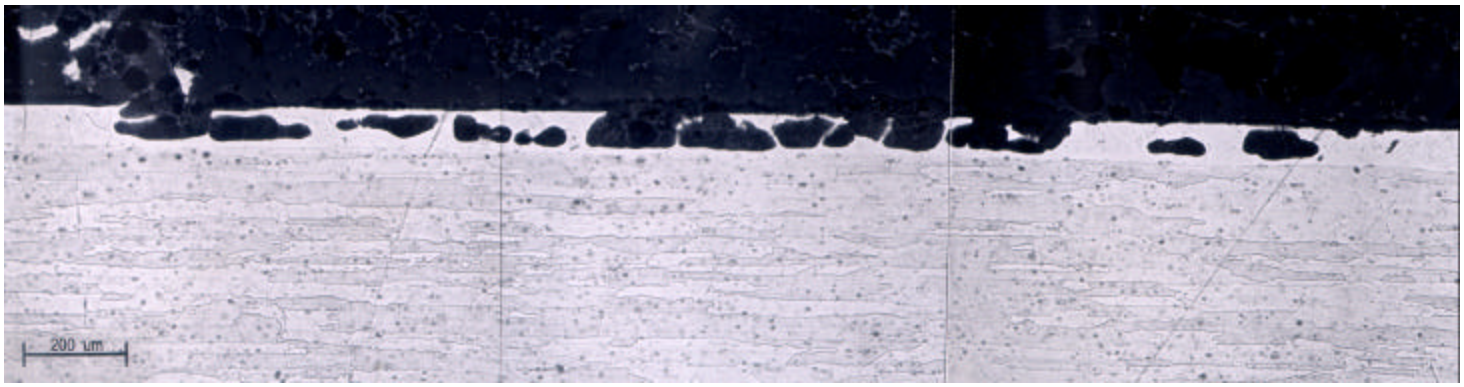

b

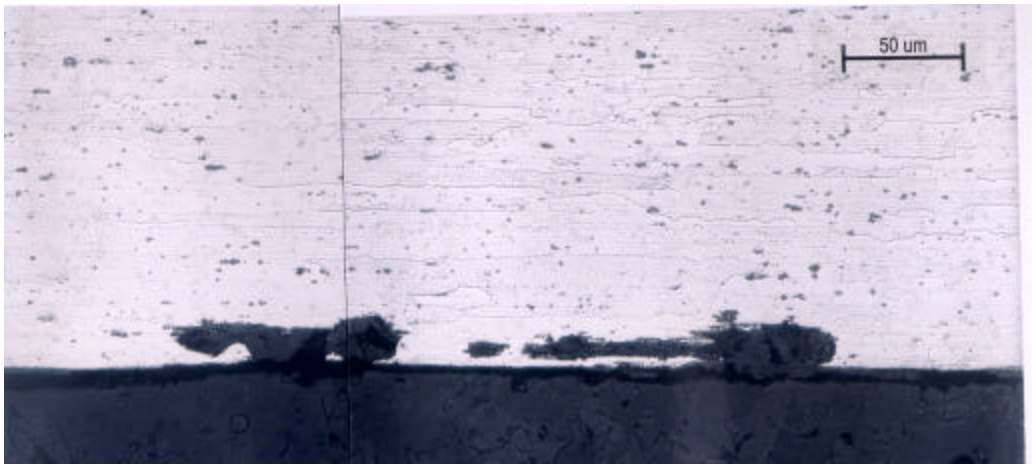

c **Etchant: Kellers**

Figure 16. Optical Micrographs of Cross Section Through Alloy 7075 Fuselage Crown Lap Joint Section

Photograph a shows pitting corrosion at a fastener hole on the outside surface. Photograph b shows corrosion of the clad layer on the outside surface. Photograph c shows pitting corrosion on the faying surface.

4.2 Microstructural Characterization

The microstructures of aluminum alloys 7075-T6, 7178-T6, and 2024-T6 that were removed from different wing and fuselage lap joints were examined and compared with similar, but recently produced alloys. The photomicrographs in Figure 17 show the microstructures of aluminum alloy 7075-T6 removed from the fuselage crown lap joint (a and b) and the recently produced alloy 7075-T6. From the micrographs, it becomes immediately obvious that the older alloy removed from the lap joints has a microstructure containing several relatively large intermetallic particles distributed throughout the microstructure. Some stringer formation as a result of processing can be seen on the lower magnification micrograph (see Figure 17b). The photomicrographs further show distinct grain boundary precipitates in the new alloy, whereas in the lap joint alloy such precipitation is not clearly marked.

Figure 18 shows optical micrographs of aluminum alloy 7178-T6 removed from the upper wing section lap joint. Although this alloy is similar to alloy 7075-T6, its microstructure appears to be different. Particularly, the grain boundaries are not clearly marked and fine precipitates occur in bands in the rolling direction. Like the 7075-T6 alloy, the alloy shows a high density of coarse intermetallic precipitates distributed throughout the alloy.

When comparing the microstructure of the aluminum alloy 2024-T3 skin with newly fabricated alloy 2024-T3, a number of differences are found. Figure 19 shows that the older skin alloy has clearly defined continuous grain boundaries, whereas the newer alloy has distinct particles marking the grain boundaries. Also, the grains of the skin alloy appear to be more equiaxed than those of the newer alloy.

4.3 Effect of Electrochemical Potential

The anodic polarization curve for 7178T6 from the fuselage crown section is shown in Figure 20. The polarization curve indicates a corrosion potential (E_{cor}) of –850 mV versus SCE. Also on this curve, two different breakdown potentials are observed, at –780 mV versus SCE and -700 mV versus SCE. Each of these breakdown potentials is characterized by a rapid increase in current density. Based on the potentiodynamic scan, alloy 7178-T6 samples were potentiostatically polarized at the two breakdown potentials for a period of 4 days. After exposure, the specimens were cross-sectioned, polished, and etched with Kellers etchant. The results of the potentiostatic tests are shown in the optical micrographs in Figures 21 and 22. The micrographs in Figure 21 show that at the first breakdown potential (-780 mV versus SCE), pitting corrosion occurred, whereas Figure 22 shows that at the second breakdown potential (-700 mV versus SCE), intergranular corrosion is the prevalent mode of attack.

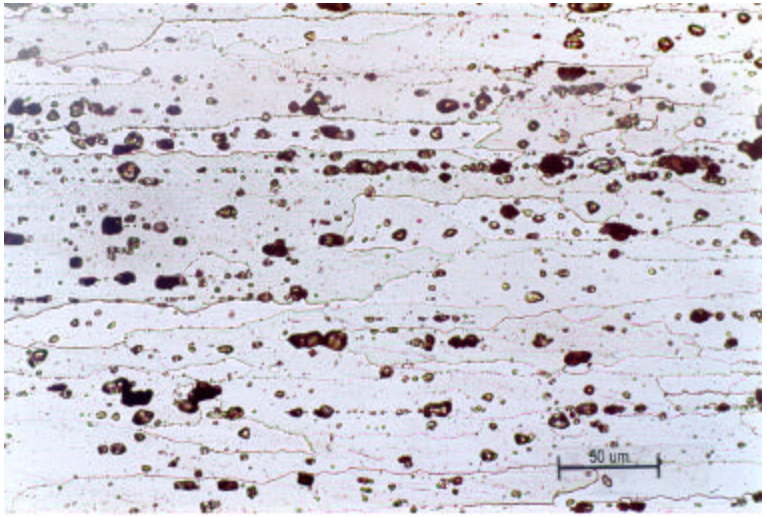

a

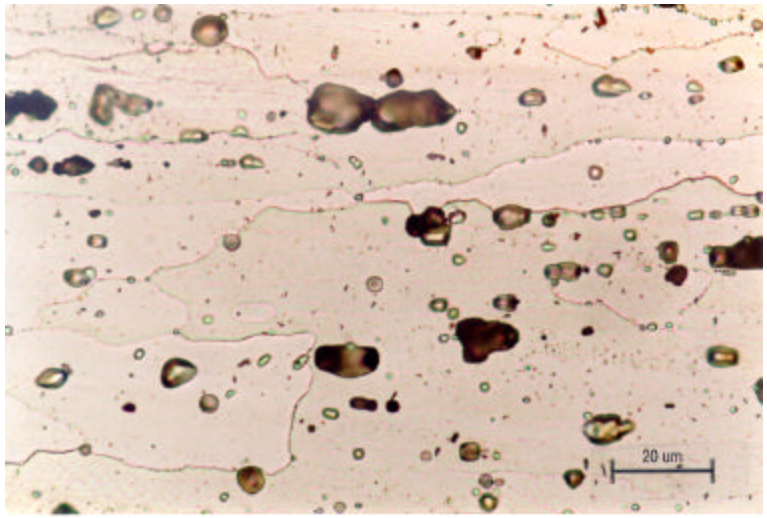

b

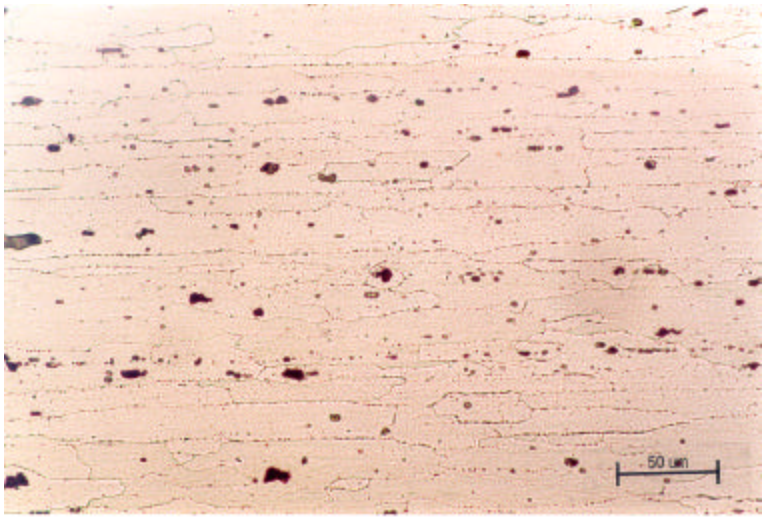

c

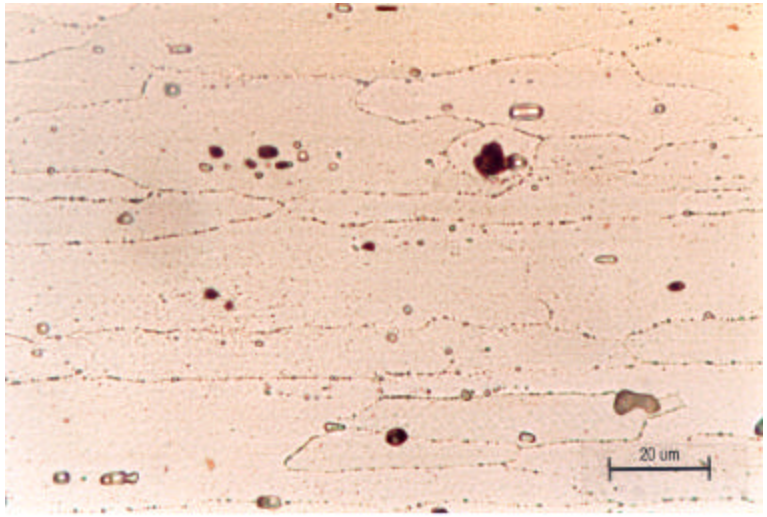

Etchant: Nitric Acid

d

Figure 17. Optical Micrographs of Aluminum Alloy 7075-T6 from the KC-135 Fuselage Crown Section (a, b) and of Recently Fabricated Material (c, d)

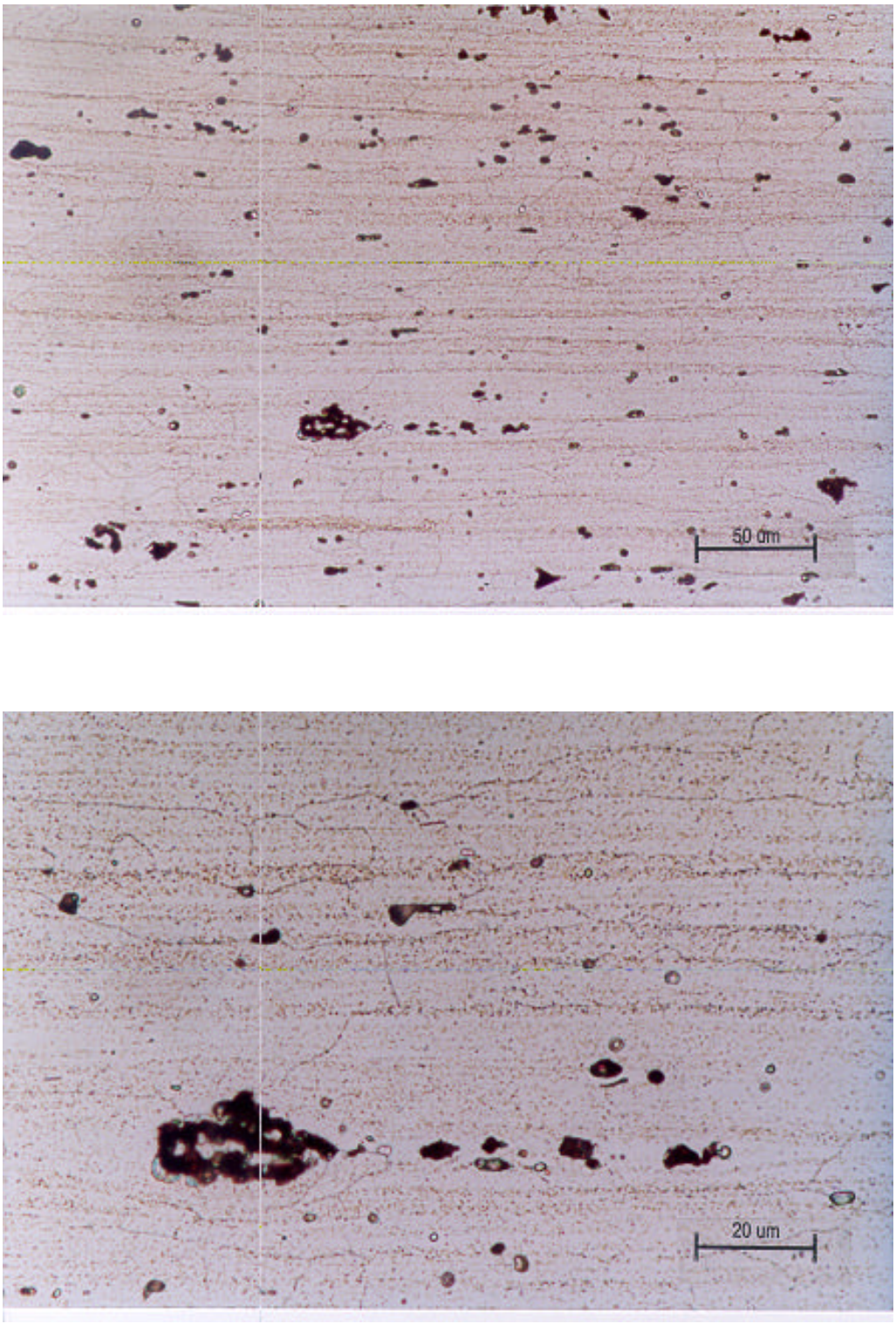

Etchant: Nitric Acid

Figure 18. Optical Micrographs of Aluminum Alloy 7178-T6 from the KC-135 Upper Wing Skin

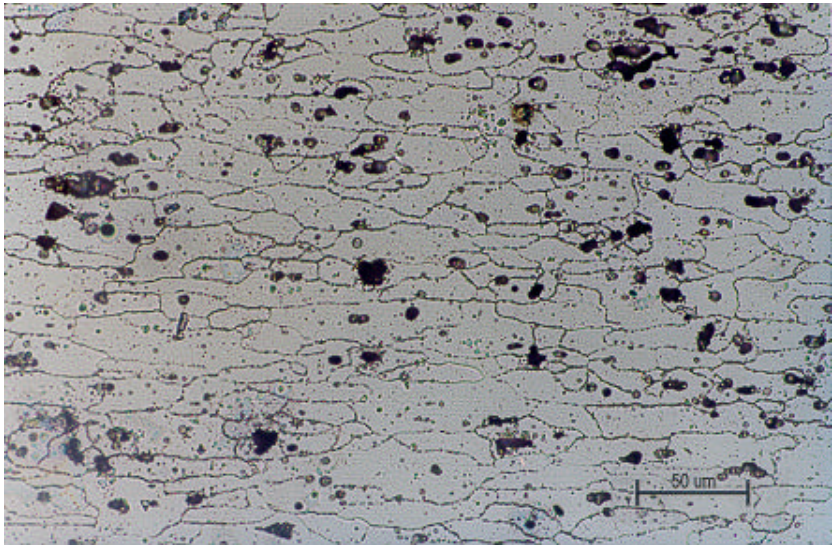

a

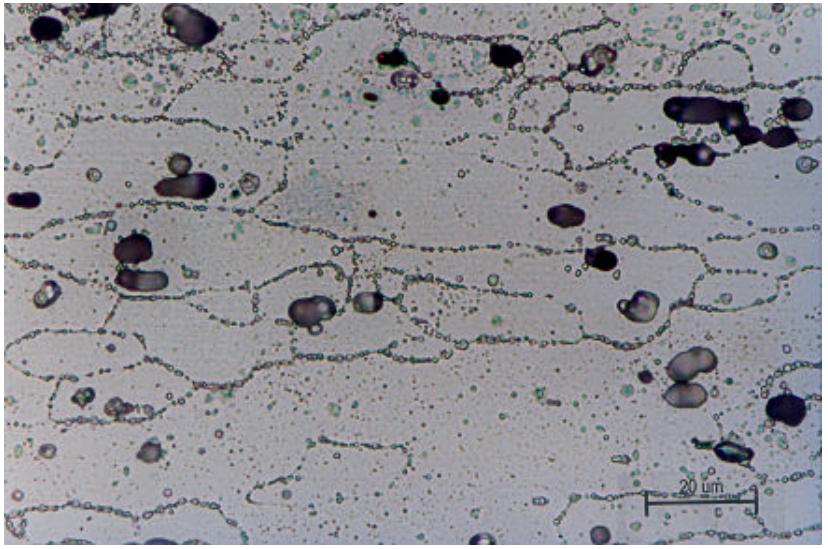

b

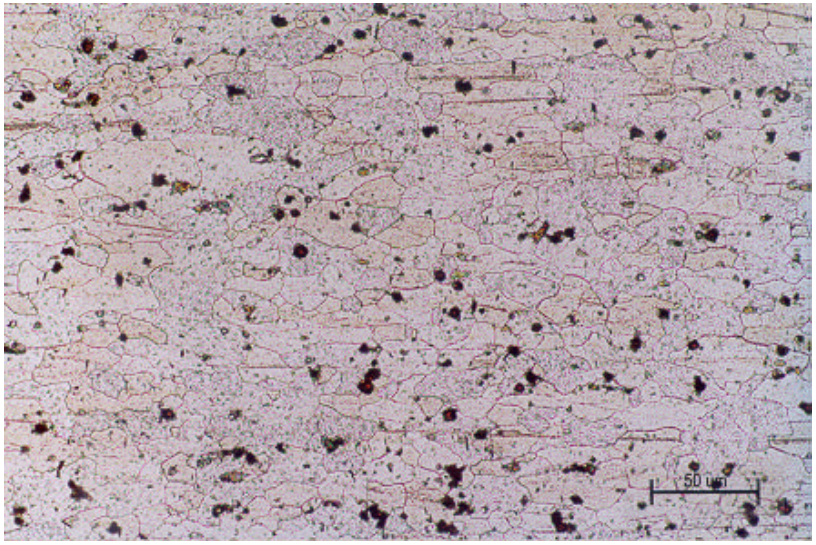

c

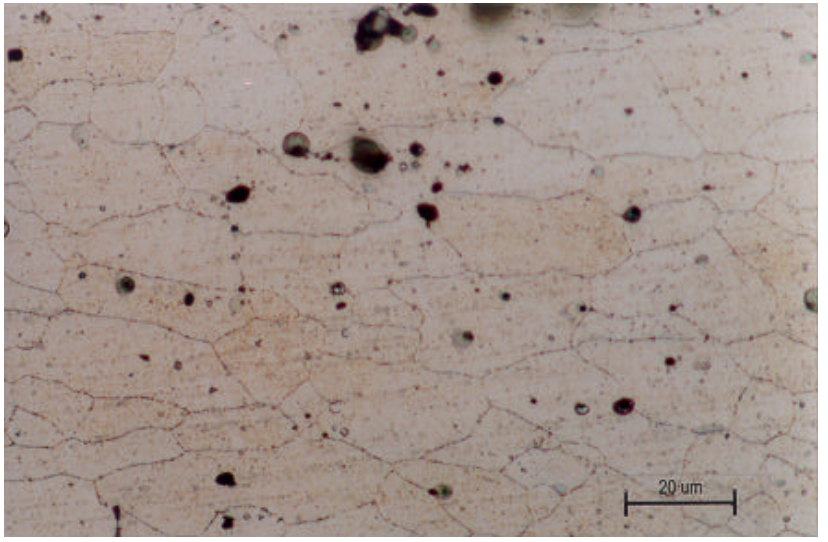

d

Etchant: Nitric Acid

Figure 19. Optical Micrographs of Aluminum Alloy 2024-T3 from the KC-135 Fuselage Skin (a, b) and of Recently Fabricated Material (c, d)

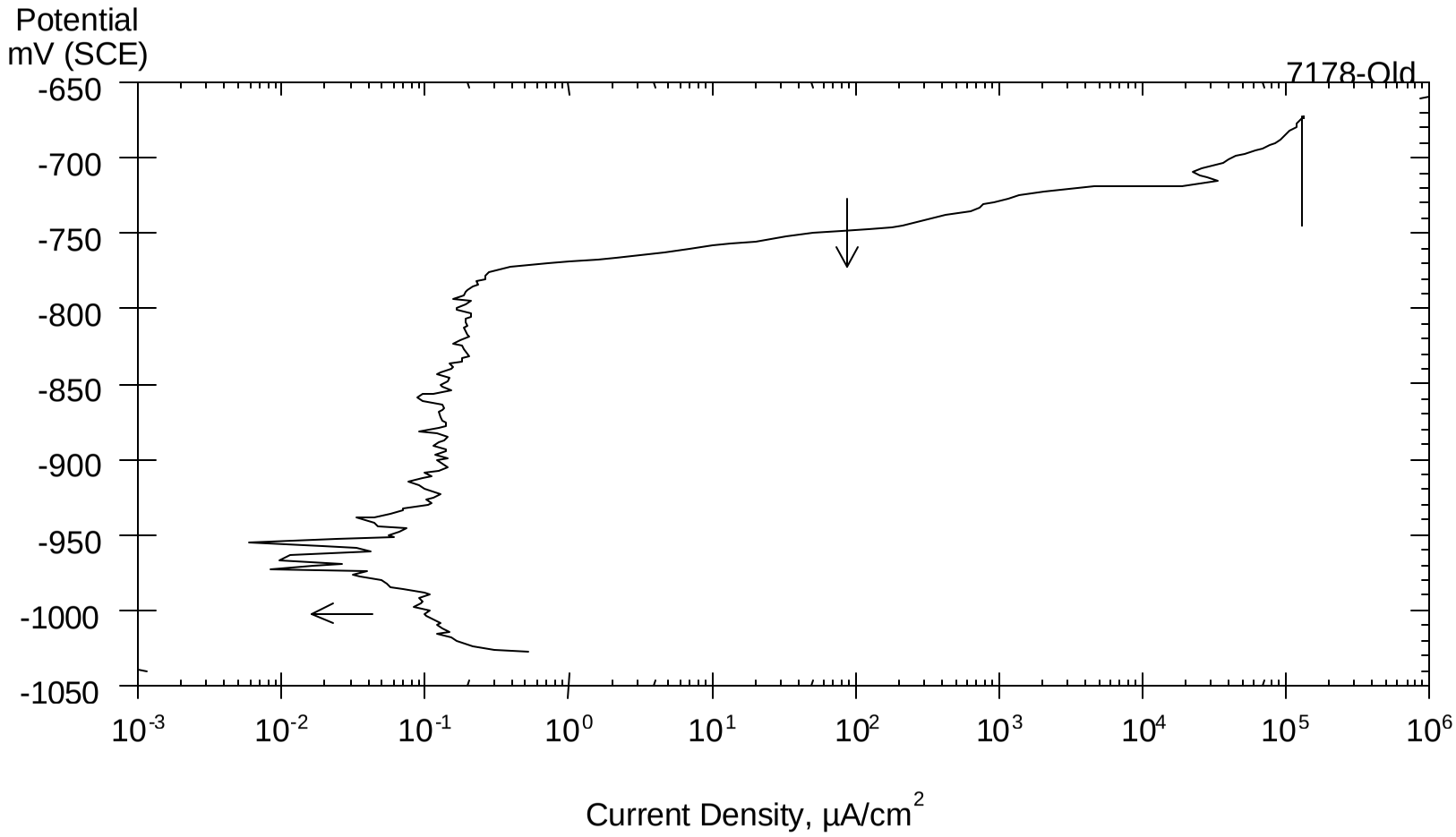

Figure 20. CPP Curve for Alloy 7178 Aluminum in Deaerated 3% (Wt) NaCl at 20°C

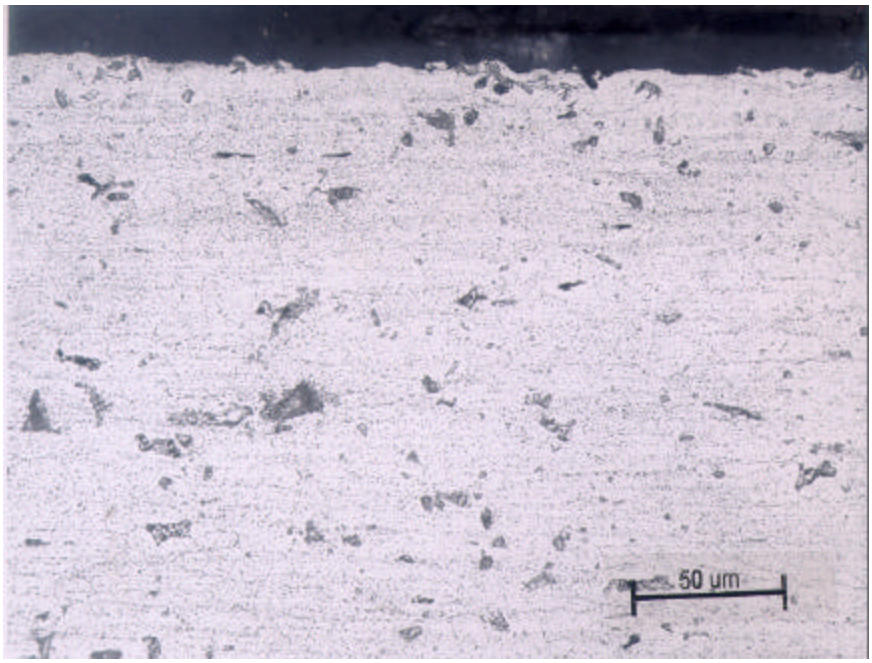

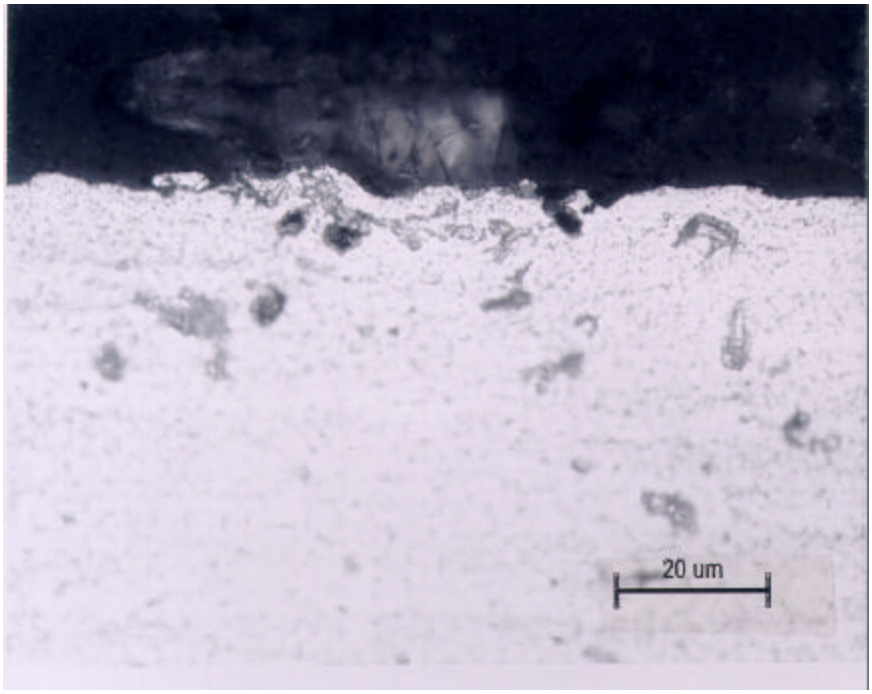

Etchant: Kellers

Figure 21. Optical Micrographs of Cross Section Through Alloy 7178-T6 after Potentiostatic Polarization at –780 mV Versus SCE, Showing Small Pits on the Surface

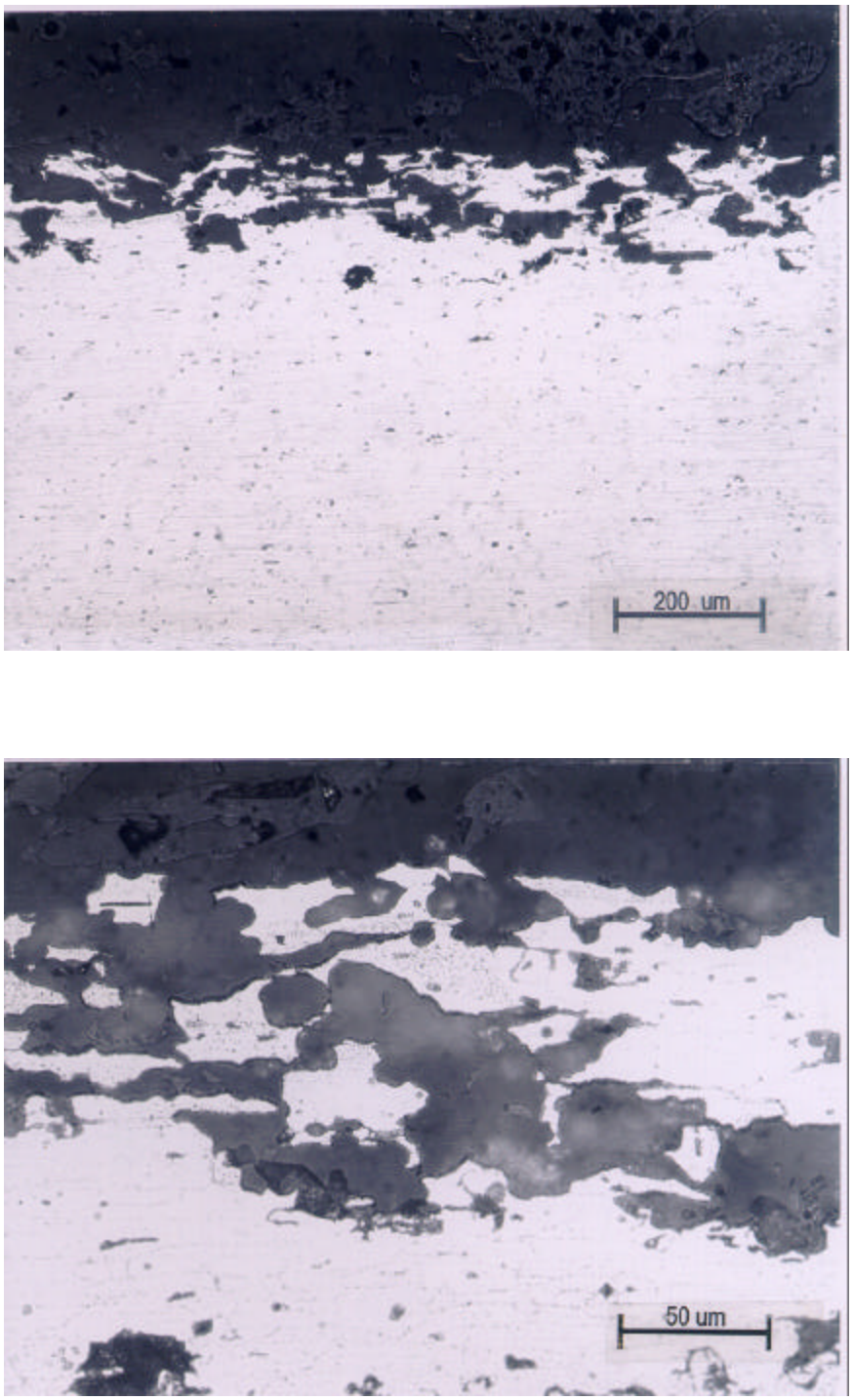

Etchant: Kellers

Figure 22. Optical Micrographs of Cross Section Through Alloy 7178-T6 after Potentiostatic Polarization at –700 mV Versus SCE, Showing Intergranular Corrosion at the Surface

5.0 DISCUSSION

The results of the metallographic examination of different lap joints of a KC-135 airplane have indicated that different forms and degrees of corrosion occur depending on the type of alloy and location on the airplane. Specifically, at one location of the alloy 7178 outboard wing section very little corrosion was found, whereas at another nearby location, extensive intergranular and exfoliation corrosion was observed. Notably, the exterior surfaces of all the sections inspected showed little or no evidence of corrosion. The only indication was the presence of grindout areas, which suggest that attempts were made to remove corrosion.

One of the outboard wing sections showed fine yet deep exfoliation corrosion around the fastener holes. The morphology of this attack was such that exfoliation could propagate without lifting the grains that would result in pillowing. The corrosion described here would result in increased stress concentration at the fastener holes, creating potential sites for fatigue crack nucleation. On the other hand, extensive exfoliation corrosion was found on the faying surface between the fastener holes. This form of exfoliation corrosion was relatively shallow, but due to corrosion of the exfoliated grains, voluminous corrosion product could form lifting the grains on the faying surface of the lap joint. The resulting pillowing effect on the stress distribution between and at the fastener holes has been described elsewhere [1-6]. Moreover, small pockets of intergranular corrosion were found under the exfoliated grains, which is consistent with previous findings [5].

Extensive corrosion was found on the alloy 2024-T3 lap joint, with copious amounts of corrosion product present inside the joint. The corrosion product had obviously resulted from corrosion of the clad layer at the faying surface. The corrosion found on the surface consisted of localized attack of clad layer which spread out laterally along the surface. The localized corrosion sites with a maximum depth of the clad layer could act as a stress concentration, and where stresses resulting from the pillowing were sufficiently high fatigue cracks could nucleate at those sites.

Little corrosion was found on the 7075-T6 fuselage crown section other than on the exterior clad layer which was nearly gone at some locations. Some pits about 25 µm deep were found on the bare faying surface.

In addition to examining the morphology of corrosion in the various lap joints, some experiments were carried out to gain insight into the effects of microstructure on the different forms of corrosion that were observed. Both 2000 and 7000 series aluminum alloys obtain their mechanical and corrosion resistance properties from precipitation hardening, which is achieved by specific heat treatment processes. For both alloys, optimal strength properties are obtained by creating coherent intermetallic precipitates in the grain. Also, as a result of these heat treatments, relatively coarse precipitates and precipitate-free zones are created along the grain boundaries and sometimes the subgrain boundaries. The compositions of these grain boundary precipitates are $CuMgAl_2$ for the 2000 alloys and $AlMgZn_2$ for the 7000 alloys. It is suspected that for the pre-1970 aluminum alloys, of which air frame components of the KC-135 are fabricated, the heat treatment was not sufficiently controlled, resulting in poor corrosion and stress-corrosion cracking resistance. When comparing the microstructures of the older aircraft alloys with those of newer alloys, significant differences were found. While in the newly fabricated 2024-T3 and 7075-T6 alloys the grain boundary precipitates consist of distinct particles, the precipitates in the older alloys appear to be more continuous. Also, the microstructures of the older alloys contain

far more coarse intermetallic or constituent particles than the newer alloys. These particles act as preferential sites for pit nucleation.

The results of the potentiodynamic polarization of alloys 7178-T6 indicate the presence of two breakdown potentials, which could be correlated with pitting and intergranular corrosion, respectively. The active breakdown potential corresponded to pitting in the matrix, while the more noble breakdown potential corresponded to intergranular corrosion. This observation is in agreement with the work of Maitra and English [7], who examined the effect of heat treatment of alloy 7075 on its anodic polarization behavior.

Further work is necessary to examine the effect of environment and electrochemical potential inside lap joints on the corrosion of alloy 7178-T6 and other pre-1970 aluminum alloys (2024-T3 and 7075-T6). Once a better understanding of these parameters is obtained, a more complete understanding of the mechanism of this form of corrosion may be developed. The results of the current work shed some light on the complex morphology of lap joint corrosion, where both intergranular and pitting corrosion can occur in close vicinity, or where pits will initially form but then change into intergranular corrosion.

6.0 CONCLUSIONS

Based on the results presented in this report, the following conclusions can be made:

1) Visual and microscopic examination of wing skin and fuselage lap joints has revealed different forms and degrees of corrosion based upon alloy type and location.
2) Often, there was little indication of lap joint corrosion on the exterior surface of the joint. Even when there were grindout marks observed on the exterior surface, indicating attempts to remove corrosion, corrosion was often found underneath those markings. This observation suggests that the practice of grinding out areas of corrosion is no guarantee of completely removing the corrosion.
3) Both pitting and exfoliation corrosion were found on the lap joint faying surfaces. Occasionally, small pockets of intergranular corrosion were found under exfoliated grains. It should be noted that even the smallest pit or pocket of intergranular corrosion (≤ 25 μm) can have a detrimental effect of the nucleation of fatigue or stress-corrosion cracks.
4) The susceptibility of the 2000 and 7000 series aluminum alloys examined in this study strongly depends on the microstructure, which depends on the heat treatment. The heat treatment of newly fabricated alloys is more controlled than that of the pre-1970 aluminum alloys, which leads to higher corrosion resistance at the same mechanical properties.
5) Anodic polarization tests have indicated different breakdown potentials for different phases in the alloy. Since the breakdown potentials are less than 100 mV apart, slight variations in environment in the lap joint could change the local electrochemical potentials and induce pitting or exfoliation corrosion.

7.0 REFERENCES

1. Bellinger N.C., S. Krishnakumar, and J.P. Komorowski, "Modeling of Pillowing Due to Corrosion in Fuselage Lap Joints," *Canadian Aeronautics and Space Journal*, Vol. 40, No. 3, September 1994, pp. 125-130.

2. Bellinger, N.C., J.P. Komorowski, and S. Krisnakumar, *Numerical Modeling of Pillowing Due to Corrosion in Fuselage Lap Joints,* LTR-ST-2005, National Research Council Canada, April 1995.

3. Bellinger, N.C. and J.P. Komorowski, "Implications of Corrosion Pillowing on the Structural Integrity of Fuselage Lap Joints," *Proceedings of the NASA-FAA Symposium on the Continues Airworthiness of Aircraft Structures*, July 1997, pp. 391-401.

4. Welch, D.W., *Fracture Mechanics Analysis of a Corroded Aircraft Fuselage Lap Joint,* Master of Science Thesis, The University of Oklahoma, Norman, OK, 1997.

5. Koch, G.H., Le Yu, and N. Katsube, "Mathematical Model to Predict Fatigue Crack Initiation in Corroded Lap Joints," *The Second Joint NASA/FAA/DOD Conference on Aging Aircraft*, Charles E. Harris, Ed., NASA/CP-1999-208982, January 1999, pp. 482.

6. Bellinger, N.C., J.P. Komorowski, and R.W. Gould, "Corrosion Pillowing Cracks in Fuselage Joints," *The Second Joint NASA/FAA/DOD Conference on Aging Aircraft*, Charles E. Harris, Ed., NASA/CP-1999-208982, January 1999, pp. 535.

7. Maitra, S., and G.C. English, "Mechanism of Localized Corrosion of 7075 Alloy Plate," *Met. Trans. A*, Vol 12A, March 1981, pp. 535-541.

8. Koch, G.H., S. Styborski, and C.A. Paul, "Corrosion Morphology in Lap Joints," *Aging Aircraft 2000*, Proc. of the 4th Joint NASA, FAA, DoD Conference on Aging Aircraft, May 2000, St. Louis, MO.

LIST OF ACRONYMS

ASTM – American Society for Testing and Materials
BS – Body Station
FEM – Finite Element Model
NDI – Nondestructive inspection (or investigation)
SCE – Saturated Calomel Electrode
SEM – Scanning Electron Microscope